THE SURFACE AND GRAIN BOUNDARY FREE ENERGIES AND THE SELF-DIFFUSION COEFFICIENT OF THE TITANIUM ALLOY Ti-5Aℓ-2.5Sn

by

WILLIAM DALE HENNING

B.S., Kansas State University, 1979

A MASTER'S THESIS

submitted in partial fulfillment of the

requirements for the degree

MASTER OF SCIENCE

Department of Chemical Engineering

KANSAS STATE UNIVERSITY
Manhattan, Kansas

1981

Approved by:

Thomas A. Fitch

Table of Contents

List of Figures and Tables

Acknowledgements

The author would like to express sincere appreciation to Dr. T. A. Roth, major professor, for his valuable suggestions and technical assistance throughout this study and constructive review of this manuscript. Appreciation also is expressed for the assistance of committee members Dr. J. C. Matthews and Dr. L. E. Erickson.

Acknowledgement of the support for the use of the scanning electron microscope by the Agricultural Experiment Station and thanks to John Krchma, operator, for his assistance is gratefully extended. Financial assistance for this study provided by the Engineering Experiment Station is acknowledged.

A special debt of gratitude is expressed to my family for their encouragement and support during the course of this study.

I. INTRODUCTION

Titanium and titanium-base alloys are becoming increasingly more important in industry, especially in the aircraft industry where higher speeds have resulted in higher skin temperatures than can be tolerated by the more common lightweight materials. The density of titanium falls approximately midway between aluminum and iron. Titanium and its alloys have a high strength to weight ratio over a wide range of temperatures. The ability to retain its strength at elevated temperatures combined with desirable toughness, thermal expansion, fatigue strength and corrosion resistance has brought titanium into significant demand. It is expected that in 1980 the shipments of titanium mill products in the U.S. will exceed the 1979 record of 19,500 tons.[1] Titanium is widely distributed around the world and is the ninth most common element in the earth's crust.

Interfacial free energies are of current technical importance industrially as well as academically. Surface and grain boundary free energies significantly influence many properties and phenomena of metals and alloys. Surface energy has been found to determine the toughness of a material breaking in a purely brittle fashion.[2] In brittle fracture accompanied by plastic flow the stress at the tip of the crack depends on surface energy.[3] A surface free energy value is required in the solution of the kinetics of sintering.[4] Interfacial energies also have important roles in coatings, depositions, oxide films,[5,6] wetting,[7] segregation or adsorption[8] and the microstructure of polycrystalline and polyphase alloys[9] as well as other phenomena.

Measuring the interfacial free energies of solid metals is difficult. Theoretical and empirical methods have generally been tedious or inadequate, often with large discrepancies between calculated and experimental values. This is mainly due to the complexity of describing decreases in electron density and translational symmetry near a surface. For the most part the theoretical and

empirical methods have dealt only with pure metals. The zero creep technique is an experimental method that has thus far provided most of the reliable values of surface and grain boundary free energies. This technique is useful only at elevated temperatures where flow of solid material can take place under small stresses. Small weights are fastened at the end of a suspended thin foil or fine wire. The weight such that no strain occurs is found, that is, the force required to balance the effects of surface and grain boundary free energies. Grooves form where a grain boundary intercepts the surface providing a relationship between the two interfacial energies. Thus two independent relationships are obtained between surface and grain boundary free energies allowing the calculation of absolute values.

In 1977 P. Suppayak[10] experimentally determined the surface and grain boundary free energies of pure titanium and the most common titanium alloy Ti-6Aℓ-4V. This study will continue that work. The objective of this study is to experimentally determine the absolute surface and grain boundary free energies and their temperature dependence of the titanium alloy Ti-5Aℓ-2.5Sn at elevated temperatures under equilibrium conditions. This information is obtained thru zero-creep of fine wires. The deformation of fine wires is assumed to be linearly controlled by a Nabarro-Herring mechanism[11,12] under experimental conditions. Assuming this mechanism, enough information is available to calculate self-diffusion coefficients. All determinations in this study are compared to literature whenever possible.

II. LITERATURE REVIEW

A. Titanium Alloys in General

Titanium is the ninth most common element in the earth's crust existing mostly as ilmenite ($FeO \cdot TiO_2$) or rulite (TiO_2). Titanium is less dense than iron or steel, non-magnetic, has lower thermal conductivity and linear coefficient of expansion and greater thermal stability and strength at elevated temperatures than either iron or aluminum.

Titanium is extremely reactive and forms a stable and protective oxide layer. As a liquid its reactivity is so great that no known refractory can be used to contain it. At elevated temperatures titanium easily absorbs oxygen, nitrogen, hydrogen or carbon interstitially contaminating and embrittling surface layers and possibly forming new compounds. It is difficult and often undesirable to produce a titanium product free from any effects from these elements. Small amounts often strengthen the alloy without significantly affecting other properties. The effects and kinetics of interactions with these materials has been discussed by McQuillan and McQuillan.[13]

Titanium as a solid can exist in two crystalline forms: alpha, a hexagonal close packed structure (hcp) or beta, a body centered cubic structure (bcc) as shown in Figure (1). For pure titanium alpha is stable below 882°C above which beta is stable to the melting point (1730°C).

Titanium alloys fall into three general structural modifications: alpha, alpha-beta and beta alloys. Alpha alloys contain largely alpha microstructure at room temperature while beta alloys contain largely beta microstructure. An alloy with a mixture of alpha and beta phases is classified as an alpha-beta alloy.

Beta alloys are characteristically responsive to age hardening, highly formable, weldable and capable of high strengths. Beta alloys contain large amounts of an alloy agent that stabilizes the beta phase to room temperature.

THIS BOOK IS OF POOR LEGIBILITY DUE TO LIGHT PRINTING THROUGH OUT IT'S ENTIRETY.

THIS IS AS RECEIVED FROM THE CUSTOMER.

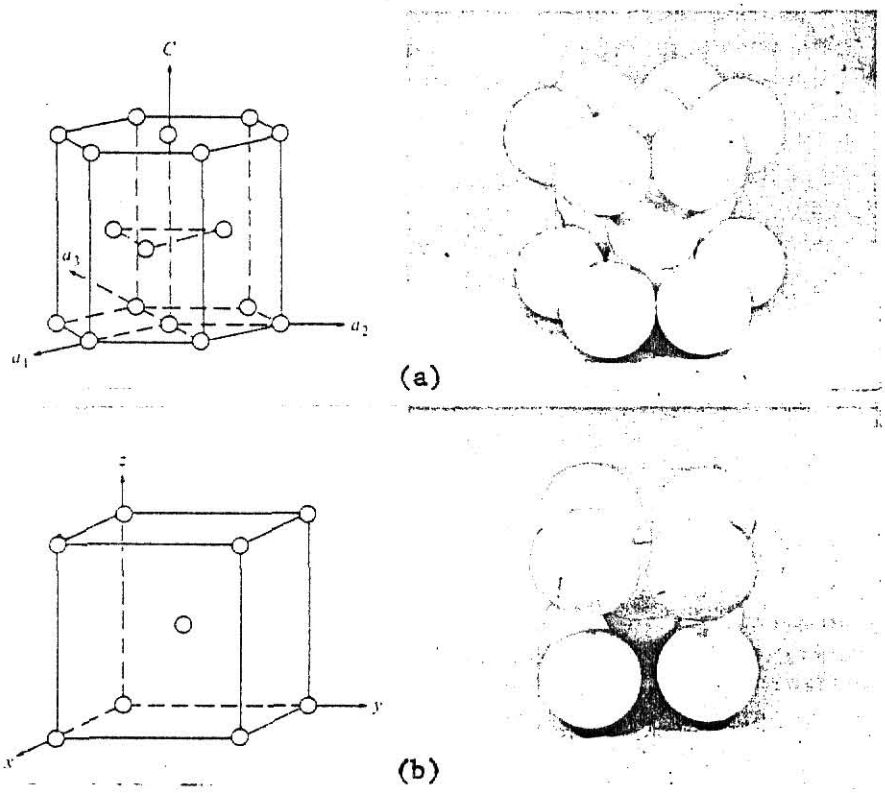

Figure (1)
The Crystalline Forms of Titanium

(a) α-hexagonal close packed (hcp)
(b) β-body centered cubic (bcc)

Taken from: R. A. Flinn and P. K. Trojan, "Engineering Materials and Their Applications", Houghton Mifflin Co., Boston (1981), p.33.

Examples of beta alloys include Ti-13V-11Cr-3Aℓ, Ti-8Mo-8V-2Fe-3Aℓ and Ti-3Aℓ-8V-6Cr-4Mo-4Zr.[14]

A number of alloying additions are more soluble in the beta phase and tend to stabilize it to lower temperatures. Such additions are termed beta stablizers. Two types of beta stabilizing additions exist: the beta eutectoid and the beta isomorphous addition.

A beta eutectoid system is illustrated in Figure (2). As the beta eutectoid addition is added the beta transus temperature is lowered until the eutectoid concentration is reached. Under certain conditions the alloy may decompose into α or β and a metallic compound as equilibrium is approached. Beta eutectoid additions such as copper and silicon are quick to decompose in solution and hence are not widely used. Additions such as chromium, iron, nickel and manganese will decompose much more slowly and are usually the most preferred of the beta eutectoids. The large majority of natural titanium deposits contain iron, some of which will appear in the final product usually as a desired impurity.

Figure (3) illustrates the beta isomorphous system. Unlike a beta eutectoid alloying addition, a beta isomorphous addition is completely miscible in the beta phase and decreases both the beta and alpha transus temperatures with increasing alloy addition. Alloy additions of this kind include vanadium, columbium, molybdenum and tantalum.

Alpha-beta alloys usually contain such alloying additions that 10 to 50 percent beta phase is stable at room temperature. These alloys have high room temperature strength but only moderate strength at elevated temperatures. They are responsive to heat treatment but generally not as formable and not at all weldable when compared to alpha or beta alloys. The alpha-beta class of alloys account for the majority of metallic titanium used. Specific alloys include

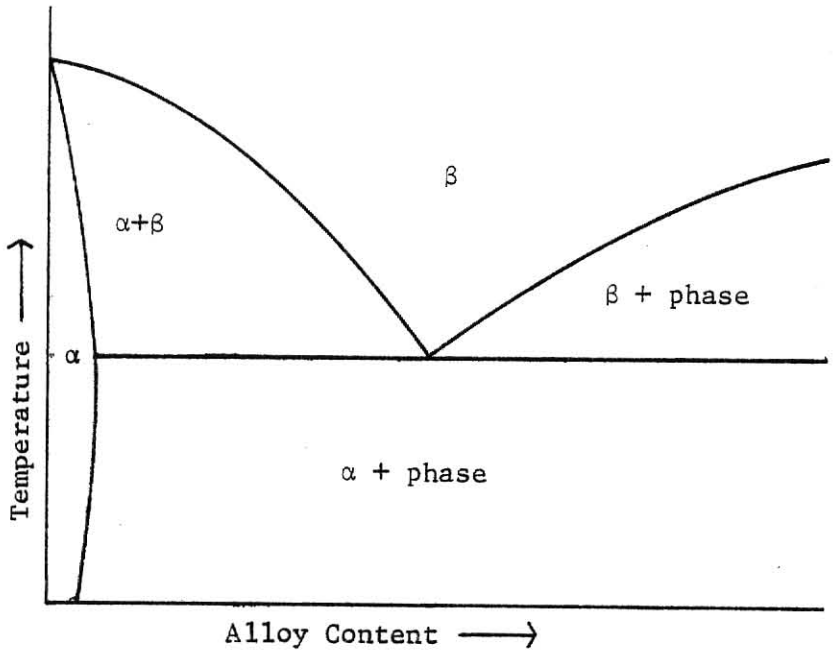

Figure (2)
Example of a Beta Eutectoid System

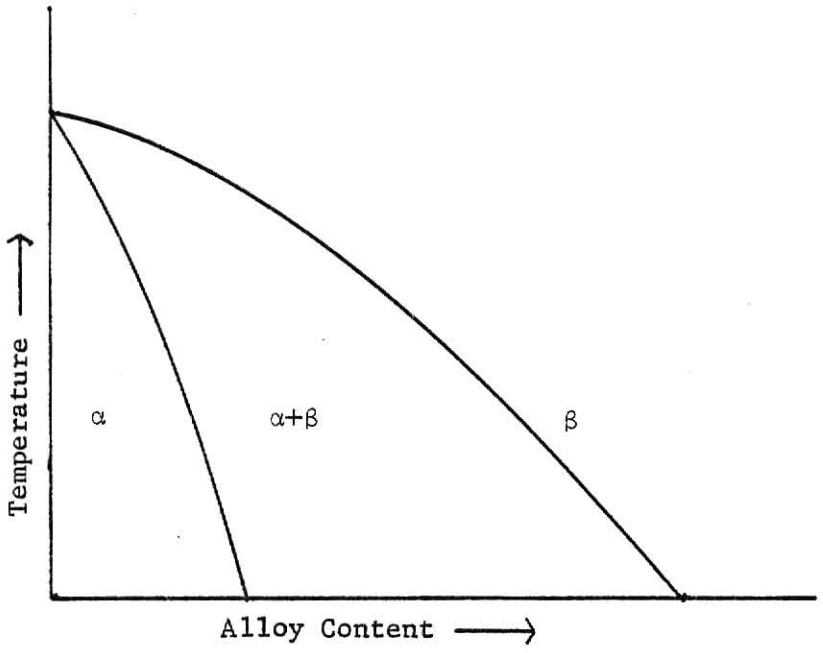

Figure (3)
Example of a Beta Isomorphous System

the most widely used titanium alloy, Ti-6Aℓ-4V, and also Ti-6Aℓ-6V-2Sn, Ti-6Aℓ-2Sn-4Zr-6Mo and Ti-3Aℓ-2.5V.[14] Alpha-beta alloys will contain various amounts of both alpha and beta stabilizers.

The alpha alloys have the highest oxidation resistance and strength at elevated temperatures. They possess the best weldability of the alloy groups and good formability, however, these alloys are usually the lowest in room temperature strength and do not respond to heat treatment. Examples include the alloy of this study, Ti-5Aℓ-2.5Sn, and also unalloyed titanium, Ti-8Aℓ-1Mo-1V and Ti-6Aℓ-2Sn-4Zr-2Mo.[14]

Alloying additions that dissolve more readily in the alpha phase and stabilize it to higher temperatures are termed alpha stabilizers. Figure (4) represents an alpha stabilized system. As the alloy content is increased both the alpha and beta transus temperature increases. Oxygen, carbon and nitrogen act as alpha stabilizers interstitially while aluminum, gallium and germanium are substitutional. Because aluminum also will decrease the density of a titanium alloy as it is added it is the most widely used alpha stabilizer.

Tin and zirconium are soluble in both alpha and beta phases and do not fall into either an alpha or beta stabilizer class. However, they do slow solid phase change kinetics and serve as strengthening agents.

B. The Titanium Alloy Ti-5Aℓ-2.5Sn

The titanium alloy Ti-5Aℓ-2.5Sn was first introduced commercially in 1953. W. L. Finlay et. al.[15] found that adding tin to a titanium alloy containing aluminum increased its strength. It was found that an alloy of 5% aluminum and 2.5% tin produced the highest strength alloy without seriously limiting fabricability. The compositional ranges of the standard and extra low interstitial (ELI) grades of Ti-5Aℓ-2.5Sn are shown in Table (1).

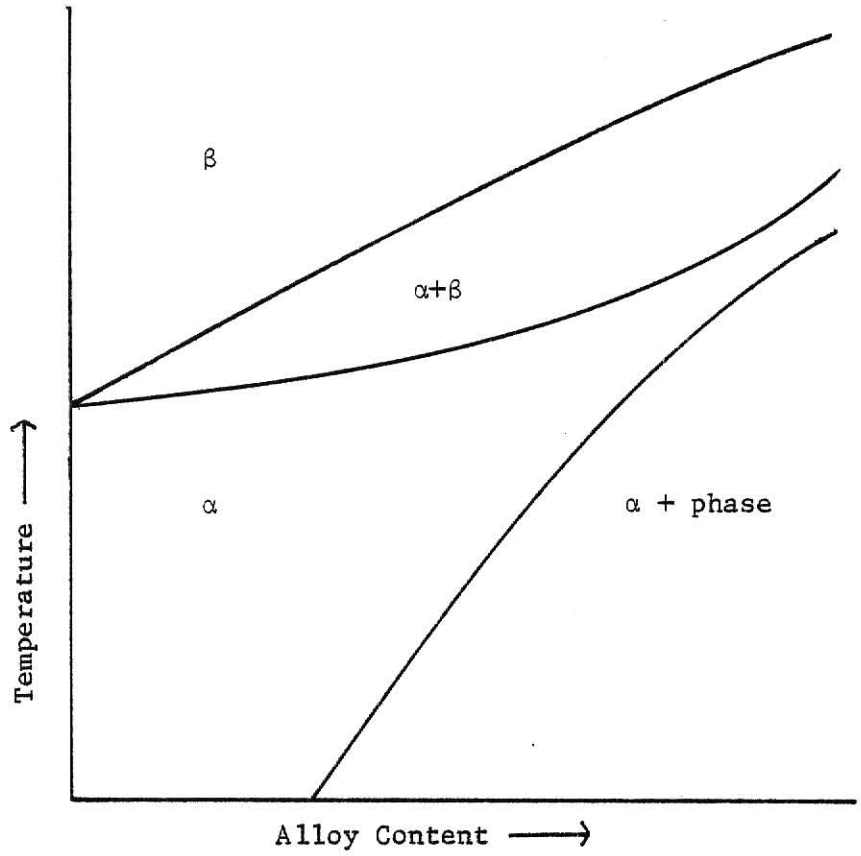

Figure (4)
Example of an Alpha Stabilized System

Table (1)
Range of Compositions of the Standard and Extra Low Interstitial Grades of the Titanium Alloy Ti-5Al-2.5Sn.*

Compositions in weight-%

	Standard Grade	ELI Grade
Al	4.0-6.0	4.7-5.6
Sn	2.0-3.0	2.0-3.0
Fe	0-0.50	0.1-0.2
Mn	0-0.30	-
O	0-0.20	0-0.12
C	0-0.15	0-0.08
N	0-0.07	0-0.05
H	0.003-0.020	0-0.0125 (bar) 0-0.0175 (sheet)
Ti	----------Balance----------	

*Taken from "Titanium Alloys Handbook", Air Force Materials Laboratory, MCIC-HB-02, December 1972.

A comparison of physical properties of various structural metals and alloys is shown in Table (2). It can be seen that the alloy Ti-5Aℓ-2.5Sn exhibits the high strength and low thermal conductivity and expansion characteristic of titanium alloys. It can also be seen that alloying titanium can significantly strengthen the material. The alloys Ti-6Aℓ-4V and Ti-5Aℓ-2.5Sn have similar properties but differ in crystalline form. The first is an alpha-beta alloy with characteristic heat treatability to high room temperature strengths and poor weldability while the latter is an all alpha alloy with good weldability, better oxidation resistance and little response to heat treatment.

Ti-5Aℓ-2.5Sn is essentially all alpha structure (hcp) below an alpha transus in the temperature range 1200-1240 K (927-967°C) and is all beta structure (bcc) above the beta transus within 1310-1365 K (1037-1092°C) to its melting point.[16] At room temperature traces of beta structure may be found due to stabilization of that phase by residual iron content. The alpha crystalline structure will exist between two basic forms shown in Figure (5): equiaxed and acicular. An equiaxed alpha structure is usually a result of mechanical working and annealing at temperatures below the alpha transus while an acicular alpha structure is produced by cooling from near or above the beta transus temperature. A moderate rate of cooling from these temperatures will produce a Widmanstatten grain structure. Extremely fast cooling produces a martensitic grain structure. Both are subcategories of acicular. Echer et. al.[17] examined the metallography of Ti-5Aℓ-2.5Sn and the effects of processing history on mechanical properties.

Typical applications of the standard grade of this alloy are as aerospace structural components such as jet engine parts, leading edges of high speed aircraft and ductwork and to a much lesser degree in chemical process industry under severe thermal or corrosive conditions. At very low temperatures very small amounts of interstitial or beta stabilizing elements will seriously

THIS BOOK CONTAINS NUMEROUS PAGES WITH DIAGRAMS THAT ARE CROOKED COMPARED TO THE REST OF THE INFORMATION ON THE PAGE.

THIS IS AS RECEIVED FROM CUSTOMER.

Table(2) Comparison of Physical Properties of Various Commercial Structural Alloys[a]

		Aℓ Alloy 2024[b]	1020 Carbon Steel[c,d]	Ti (40 ksi grade)[b]	Ti-6Aℓ-4V[b]	Ti-5Aℓ-2.5Sn[b]
Density @ 298K (kg/m^3)		2770	7860	4510	4470	4460
Melting Point or Range (K)		775-910	1780-1800	1940	1810-1920	1810-1920
Ultimate Yield 0.2% dev. (N/m^2)	@ 298K	$2.1(10^8)$	$4.2(10^8)$	$4.1(10^8)$	$9.0(10^8)$	$9.0(10^8)$
	@ 673K	$1.2(10^8)$	$4.6(10^8)$	$2.3(10^8)$	$7.2(10^8)$	$6.6(10^8)$
Yield Strength 0.2% dev. (N/m^2)	@ 298K	$0.83(10^8)$	$2.6(10^8)$	$2.8(10^8)$	$8.6(10^8)$	$8.4(10^8)$
	@ 673K	$0.62(10^8)$	$2.2(10^8)$	$1.5(10^8)$	$6.9(10^8)$	$5.7(10^8)$
Coefficient of Linear Expansion 298 to 373K (1/K)		$23(10^{-6})$	$12(10^{-6})$	$9.0(10^{-6})$	$9.4(10^{-6})$	$9.4(10^{-6})$
Thermal Conductivity @ 298K (W/mK)		130	52	16	6.9	7.3
Specific Heat @ 298K (J/kgK)		840	420	530	520	520

[a] All Properties for commercial grade materials annealed.

[b] "Aerospace Structural Metals Handbook", vol. 2, Air Force Materials Laboratory, AFML-TR-68-115 (1971)

[c] E.R. Parker, "Materials Data Book", McGraw-Hill, New York (1967)

[d] "Elevated-Temperature Properties of Carbon Steels", ASTM, Philadelphia (1955)

THIS BOOK CONTAINS NUMEROUS PICTURES THAT ARE ATTACHED TO DOCUMENTS CROOKED.

THIS IS AS RECEIVED FROM CUSTOMER.

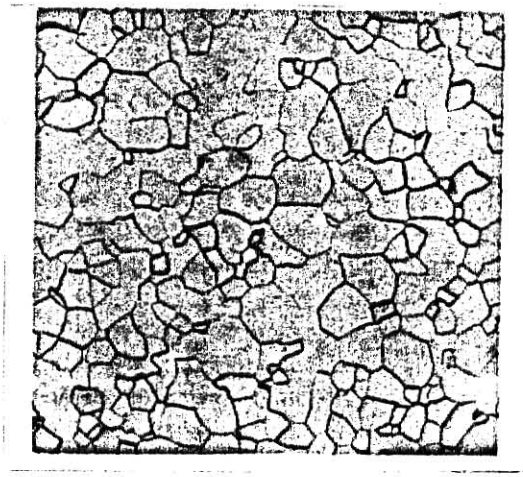

(a) X100

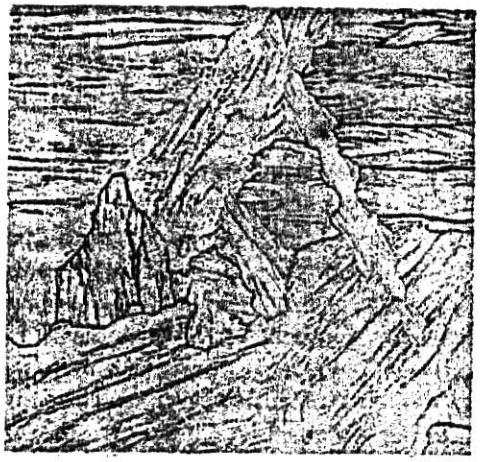

(b) X100

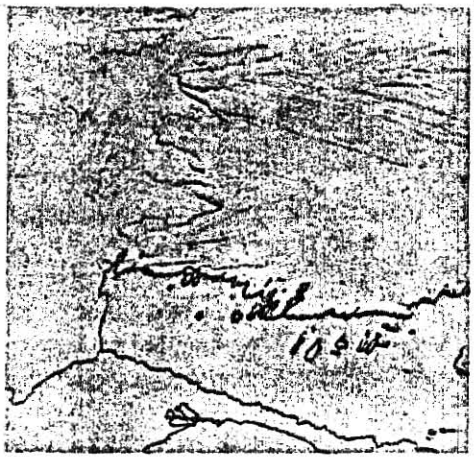

(c) X100

Figure (5)
The Basic Grain Structures of Alpha Titanium

(a) Equiaxed Alpha
(b) Acicular Alpha / Widmanstatten
(c) Acicular Alpha / Martensitic

From: "Titanium Alloys Handbook", Air Force Materials Laboratory, MCIC-HB-02(1972), section 1.

embrittle the alloy that would otherwise have very little effect. Thus, under cyrogenic conditions the ELI grade is used. This grade is widely used for low temperature storage vessels because of its high strength to weight ratio and toughness under these conditions and ease of fabrication.

C. Interfacial Energy

Surface energy in a solid metal may be visualized as follows. Within the interior of the metal each atom is surrounded and bonded to, say, Z_i neighbors. An atom on the surface is only partially surrounded by $Z_s < Z_i$ neighbors. On bringing an atom from the interior to the surface $Z_i - Z_s$ bonds must be broken and others may be distorted, thus there is an increase in free energy. Also contributing to the interfacial free energy are effects from a longer range than nearest neighbors. Surface free energy (λ_s) may be defined as the reversible increase in free energy per unit area of new surface formed. Grain boundaries also involve the breakage and distortion of interatomic bonds and may be visualized in the same way.

For the most part empirical and theoretical approaches to surface and grain boundary free energies of metals have been inadequate often with large discrepancies with experimental results. These approaches have almost exclusively been applied to pure metals, rarely to alloys. Empirical methods[18-30] have sought to determine interfacial free energies of solid metals as a function of physical properties such as surface work functions, density, heat of fusion, crystalline structure and orientation, and modulus of elasticity. Recently a Monte Carlo simulation of a grain boundary was presented by R. Chang.[31] Using copper as an example, Chang was able to predict grain boundary free energies that compared favorably with experiment. Theoretical approaches[32-40] generally must treat interfaces in terms of electron-ion and electron-electron

interactions. An electron density for an appropriate pseudopotential model must be calculated at the interface. Theoretical and empirical considerations of interfacial energies continue to be ongoing fields of study.

At best it is difficult to measure surface and grain boundary energies accurately. Experimental methods have been reviewed by Murr[41] and Inman and Tipler[42] and earlier by Udin,[43] Hess[44] and Fisher and Dunn.[45] The only experimental technique of consequence is known as zero creep, first used by Sawai and Nishida[46] and Tamman and Boehme[47] later modified by Udin et. al.,[48] Udin,[49] Pranatis and Pound[50] and Hondros.[51] Zero-creep has been widely accepted though repeatably opposed by Bikerman.[52-54] The technique uses very thin foils or fine wires heated to temperatures near the melting point. The technique was developed from observations that a metal sample with a large surface to volume ratio heated to temperatures near its melting point will tend to shrink, that is, the surface tension will exceed the static stress associated with the weight of the sample.

D. Zero Creep in Fine Wires

Typically, the zero creep method uses samples in the form of a thin rectangular foil or a fine cylindrical wire. Both shapes have a high surface to volume ratio. The fine wire is usually preferred because it is easier to describe grain boundaries in the geometry of the wire and the stress system is simpler.

The zero creep technique does not actually measure interfacial free energy but measures interfacial tension. Shuttleworth[55] has shown that generally for a solid,

$$\sigma_i = \lambda_i + A_i \frac{d\lambda_i}{dA_i} \qquad (1)$$

where: σ_i = tension of interface "i"

λ_i = free energy of interface "i"

A_i = area of interface "i"

For a liquid or a solid at temperatures near its melting point an interface is able to migrate thru diffusion so that the number of atoms per unit area of interface would tend to be constant. For a liquid it is known for an isothermal deformation at constant volume the second term on the right side of equation (1) is zero because atoms will be continuously transferred to the surface to maintain a constant surface concentration. For a solid near its melting point it has been shown to be physically impossible for that term to be identically zero,[56] however, it is negligible compared to λ_i.

Using the zero creep method fine wires with diameter < 1mm are prepared. Small weights are attached to the free end and the wire is knotted or scribed in intervals of ∿2cm to serve as gauge marks. The wire is hung in a furnace tube and annealed at or above the test temperature in vacuum or inert gas atmosphere for an initial period of 10 to 30 hours, then the wires are cooled and straightened if necessary prior to the first measurement of distance between gauge marks. At this point the intersections of free surface and grain boundary will usually present itself as thermally etched grooves as shown in Figure (6). These grooves effectively immobilize the grain boundaries so that no grain growth will occur in further creep test. Chalmers, King, and Shuttleworth[57] described this thermal grooving at the intersection of surface and grain-boundary interfaces as a condition of interfacial free energy minimumization. Udin[43] suggested that the grains have recrystallized and grown to an equilibrium shape during the initial anneal. The wires are then brought to and held at test temperature for a period of time, usually 50 to 200 hours. Gravitational forces will tend to elongate the wires while surface forces tend

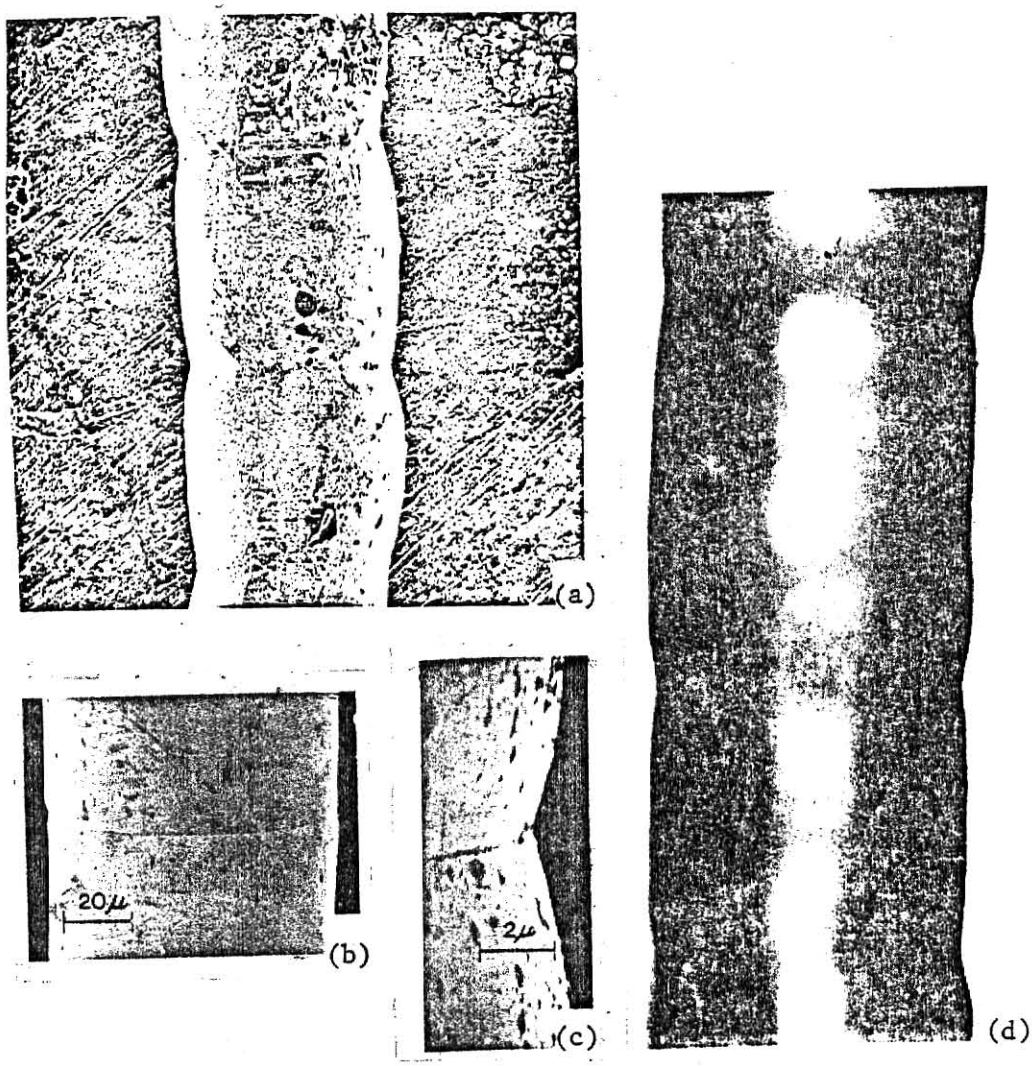

Figure (6)
Examples of Grain Boundary Grooves
in Fine Wires

(a) Scanning Electron Micrograph of Titanium Annealled at 1200°C (P. Suppayak, "The Surface and Grain Boundary Free Energies of Pure Titanium and the Titanium Alloy Ti-6Aℓ-4V", Masters Thesis, Kansas State University (1977).)

(b) and (c) Scanning Electron Micrograph of Nickel Annealled at 1060°C (L. E. Murr, O. T. Inal and G. I. Wong, "Electron Microscopy and Structure of Materials", University of California Press, Berkeley (1972), pp. 417-26.)

(d) Optical Micrograph of Iron Annealled at 1480°C (T. A. Roth, Mat. Sci. and Engg., 18 (1975), 183.)

to shorten them. The wires are then cooled and the change in gauge lengths determined. The strain, ε, of each wire is defined as:

$$\varepsilon = \frac{(\ell - \ell_o)}{\ell_o} \tag{2}$$

where: ℓ_o = initial gauge length

ℓ = final gauge length

It has been shown[42,50,58-60] that the creep of fine wires under these conditions is linearly controlled by a Nabarro-Herring mechanism.[11,12] Nabarro and Herring independently theorized that solid metals could deform under low stresses by a self-diffusion mechanism. Under such a mechanism a plot of elongation versus time would be linear, that is, a constant creep rate. Also, elongation versus stress would also be linear within a reasonable range. They suggested that vacant lattice sites diffuse thru the crystal with grain boundaries and free surfaces serving as vacancy sources and sinks. Mass transfer would occur in the opposite direction of vacancy flow. The self-diffusion coefficient, D, for this mechanism was found to be:

$$D = \frac{2\varepsilon\bar{\ell}rRT}{t\beta U\sigma} \tag{3}$$

where: $\bar{\ell}$ = mean grain length

r = wire radius

R = gas constant

T = absolute temperature

t = time of creep

β = a constant, $\simeq 12$ when $\bar{\ell} \geq 2r$

U = volume per mole of atoms

σ = stress on the wire

It was assumed that the grains occupy the entire wire cross-section and are perpendicular to the wire axis.

H. Jones[61] compared self-diffusion coefficients determined from creep data to those determined from radiotracer data for several solid metals. It was found that self-diffusion coefficients calculated from reliable radiotracer values were much smaller than those calculated from creep data that involved relatively short creep durations. However, reasonable agreement was obtained when:

$$\frac{D_r t}{2r\bar{\ell}} \gtrsim 3 \tag{4}$$

where: D_r = radiotracer estimate of the self-diffusion coefficient

H. Jones postulated that the discrepancies resulted from a transient effect of dislocations acting as vacancy sources or sinks.

From the definition of interfacial energy it can be written that at constant temperature:

$$\lambda_s \, dA_s + \lambda_{gb} \, dA_{gb} = f d\ell \tag{5}$$

where: λ_s = surface free energy

dA_s = differential change in surface area

λ_{gb} = grain boundary free energy

dA_{gb} = differential change in grain boundary area

f = static force due to gravity

$d\ell$ = differential change in the wire length

That is, an infinitesimal change in the total surface and grain boundary energies is equal to the work done on or by the weight of the sample. For a fine cylindrical wire, ignoring end effects, the surface energy will act

over the area $2\pi r\ell$ and the grain boundary energy will act over the area $n\pi r^2$ where n is the number of grain boundaries. It should be noted that the grain boundaries are assumed to be aligned perpendicular to the wire axis. Then for constant volume ($V = \pi r^2 \ell$):

$$dA_s = 2\pi d(r\ell) = \frac{\pi V}{\ell} d\ell \tag{6}$$

$$dA_{gb} = \pi n d(r^2) = - n V/\ell^2 \, d\ell \tag{7}$$

Substituting equations (6) and (7) into equation (5) and replacing V the following is obtained:

$$f_o = \pi r(\lambda_s - r(\tfrac{n}{\ell})\lambda_{gb}) \tag{8}$$

where: f becomes f_o, the balance load at zero strain.

The effective load of each gauge length is determined by cutting the wire at the midpoint of each gauge length and weighing the wire and weight below that point. The balance load at zero strain, f_o, is determined from a linear regression line of a plot of effective load versus strain as typified in Figure (7).

After a sufficiently long anneal a groove will form where a grain boundary intercepts a free surface to form a bamboo-like structure as shown in Figure (8). At equilibrium the surface and grain boundary free energies can be related by a statement of force equilibrium:

$$\lambda_{gb} = 2\lambda_s \cos(\Omega/2) \tag{9}$$

where: Ω is the measured groove angle

Smith[62] has shown that the measured groove angle is characteristic of the interfaces involved. Substituting equation (9) into equation (8) and solving for the surface free energy gives:

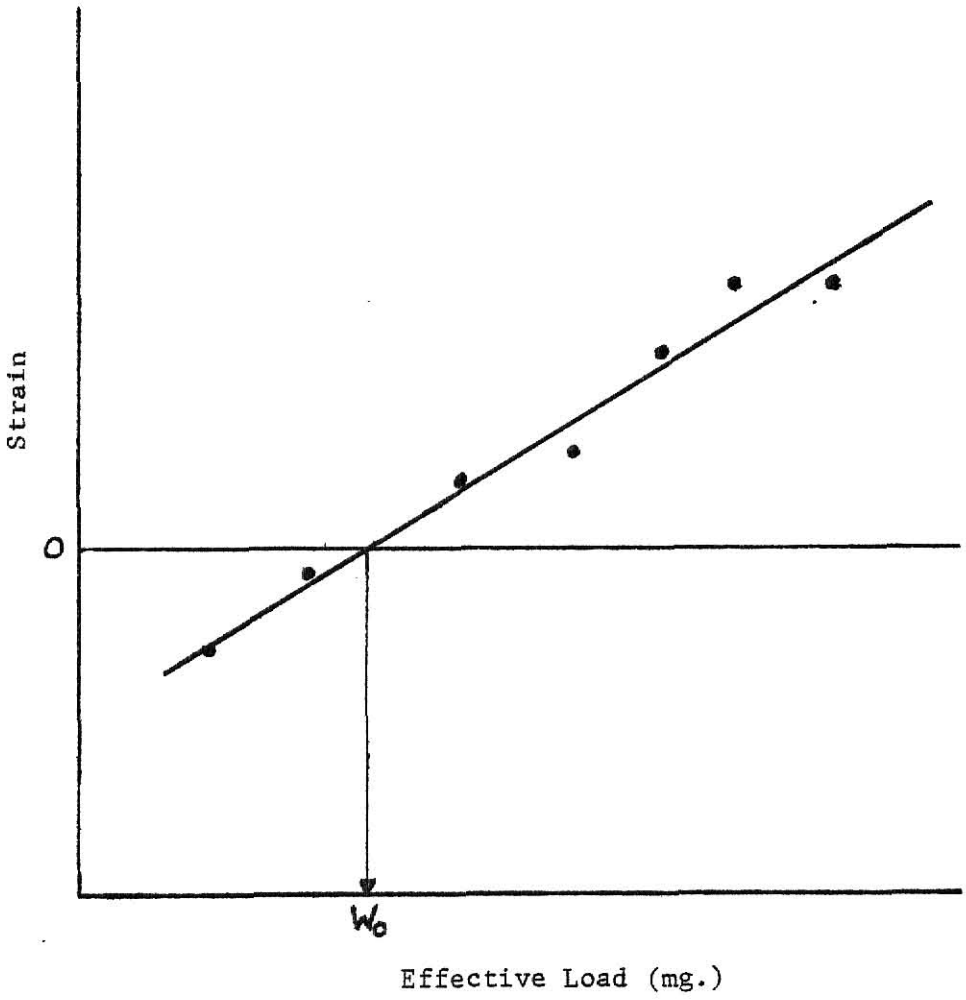

Figure (7)
Typical Example of Linear Regression Between Elongation and Effective Load to Find the Balance Load: $f_0=W_0g$ (Where g= acceleration due to gravity).

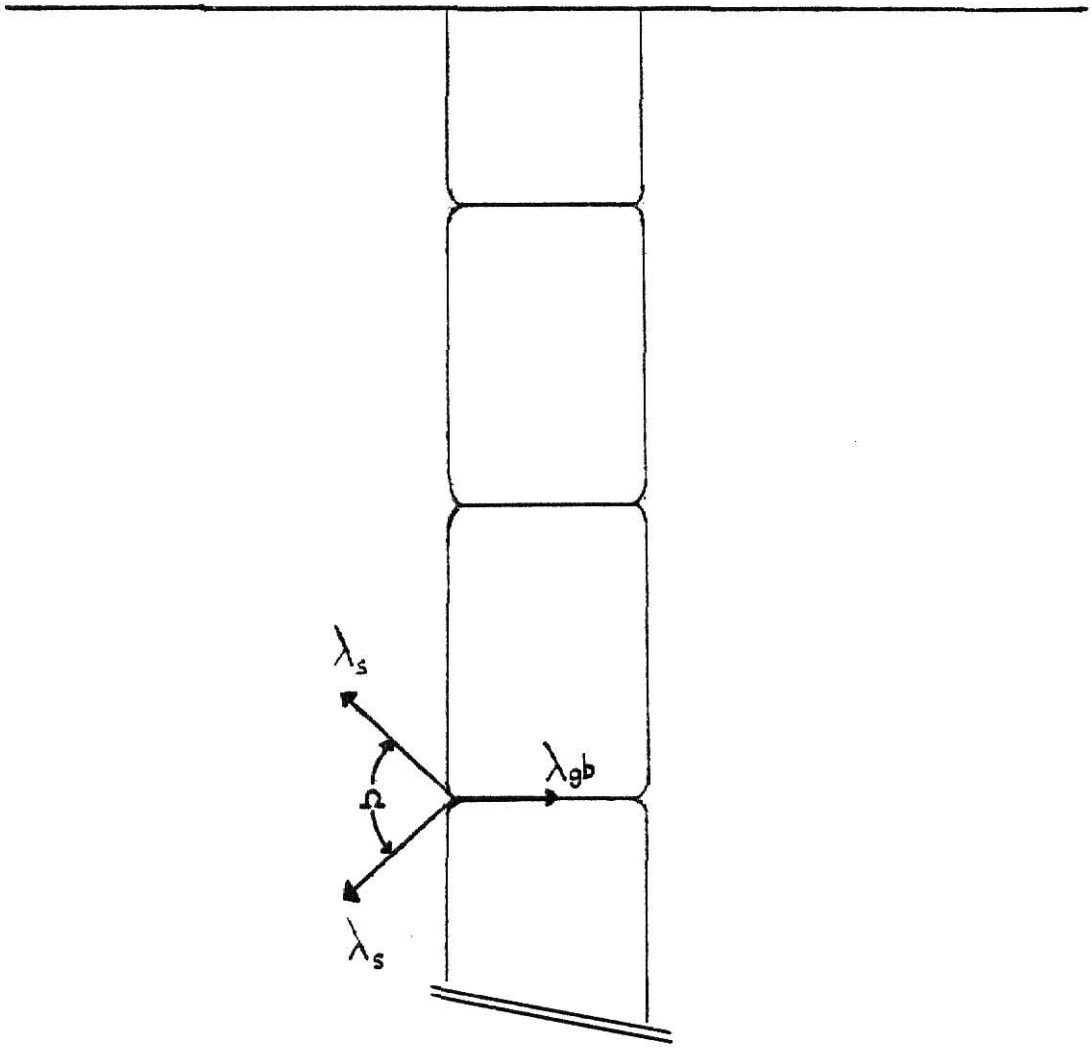

Figure (8)
Diagram of Bamboo Structure Caused by Thermally Etched Grain Boundary Grooves in a Fine Wire Crept at High Temperature

$$\lambda_s = \frac{f_o}{\pi r(1 - 2r(n/\ell)\cos(\Omega/2))} \tag{10}$$

This study measures average surface and grain boundary free energies. That they are anisotropic is a well known fact thru both thermodynamics[63-65] and experiment.[66-68] However, Reigger and Van Vlack[69] has shown that the median angle of relatively few observations is close to the true dihedral angle.

Substitution of experimental parameters into equations (10), (9) and (3) will give absolute values of the average surface and grain boundary free energies and the self-diffusion coefficient of the specimens for each creep test.

III. Methods and Materials

A. Methods

In general the results of this study were obtained in a two step procedure. First, the balance load was determined in which the static stress due to gravitational forces equaled forces associated with interfacial tensions. Second, the angles of thermally etched grain boundary grooves at equilibrium with the surface were measured. Information from both these steps was required to obtain absolute values of the surface and grain boundary free energies.

Sample preparation occurred as follows. A length of the fine wire was cut from a reel. A loop was tied at one end and small overhand knots were tied along the length of the wire in intervals of between 2 and 5 cm, usually near 3 cm, to serve as gauge markers. A small titanium weight was tied on the end opposite the loop. The mass of this weight was comparable to that used by Roth and Suppayak[70] for pure titanium and the titanium alloy Ti-6Aℓ-4V. Ideally, the mass of the weight would be near the balance load in order to achieve greater accuracy. An example of a prepared sample is sketched in Figure (9). Finally, the wire was washed in ethanol and acetone to remove any dirt or oils due to handling.

Two wires per test were suspended from a titanium holder in a vertical furnace tube and sealed from the air. Prior to heating, the system was evacuated and flushed with dried high purity helium several times to insure that no oxygen or nitrogen would be present to contaminate the surface of the speciman. Heating was carried out in this atmosphere at slightly above room pressure not only to prevent surface contaminations but also to avoid sublimation problems. The wires were initially annealled at or above test temperature for 24 hrs.

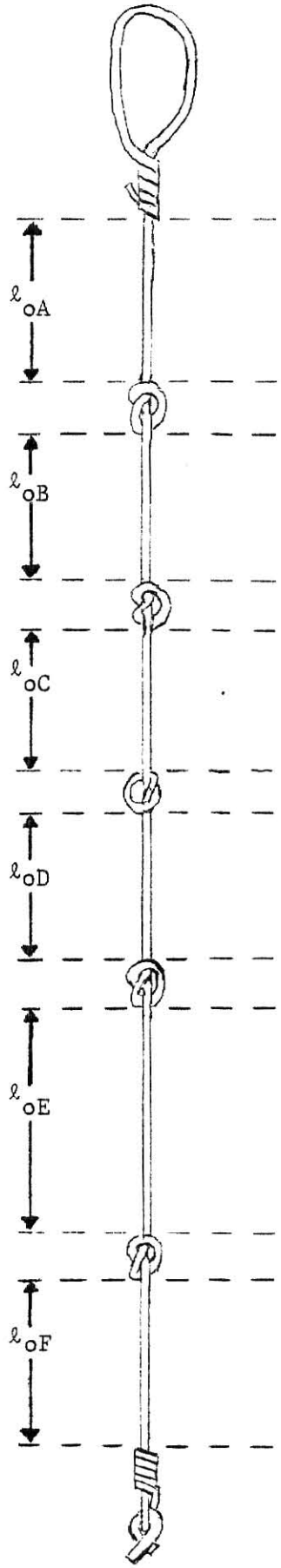

Figure (9)
Diagram of Typical Prepared Wire Specimen

Typical Gauge Length: $\ell_o \cong$ 3cm.
Typical Overall Length: $L \cong$ 25cm.
Size of Gauge Knot: $<$ 0.25cm.
Wire Diameter: d= 0.102mm.

After cooling from the initial anneal it was generally observed that the grains had grown to apparent equilibriun size and configuration and often thermally etched grooves appeared. The initial anneal also served to straighten the wires. The knots which acted as gauge markers would sinter at the elevated test temperatures and thus would not take part in future creep of the sample. At this point the first measurement of the gauge lengths was performed.

The samples were then again hung in the furnace tube for the creep anneal, again flushing the system several times with dried helium. The samples were heated to test temperature and held usually for a duration near 96 hrs. During this period the wire would shrink or lengthen under a Nabarro-Herring mechanism.

Upon cooling and removal from the furnace tube the wire samples were found to be bright and ductile and believed free of surface contamination. The number of grains in each gauge segment was counted as the final gauge length measurements were performed. Strain for each segment was then calculated using equation (2).

After measurement, each segment was accurately cut at its midpoint and the mass of the entire sample below a particular segment was recorded as its effective load. A least squares linear fit between strain and effective load was then applied to find the balance load as exemplified previously in Figure (7).

Examination of the wires under a microscope revealed the desired bamboo structure. Numerous grain boundary grooves were photographed using a scanning electron microscope (SEM). The photographs were enlarged prior to the measurement of the groove angles. The median angle was taken as the desired value for that test. Magnification was high enough to ensure that the angle was measured from its root. Use of SEM over other means of recording groove

angles was preferred because of its high resolution and depth of field. Applications of electron microscopy in studies of metal interfaces have been presented by Murr, Intal and Wong.[71]

Finally, the necessary experimental values were substituted into equation (10) and then into equation (9) to calculate the surface and grain boundary free energies determined for that test.

B. Materials

The wire used was 0.102 mm (0.004 in.) in diameter obtained commercially from Aeromet, Inc. Its composition, shown in Table (3), falls within the standard grade of Ti-5Aℓ-2.5Sn.

A Lindberg high temperature verticle tube furnace heated by electrical resistance was used in this study. Temperature was controlled with an indicating and controlling potentiometer connected to Pt/Pt·13%Rh thermocouples. The furnace was equipped with removable alumina furnace tubes. Each tube was heated while being evacuated for at least 24 hrs. prior to use to remove any possible contaminates and then is used only for one particular type of alloy. A diagram of the furnace system is shown in Figure (10). Evacuation was performed by a mechanical vacuum pump. A microsieve trap was employed to remove any water vapor that might be present in the purified helium supply.

Gauge length measurements were made by a Gaertner micrometer microscope with filar eyepiece mounted on a horizonally travelling stage capable of measuring to $\pm$ 1.27 μm ($\pm$ 0.00005 in.) within a full scale of 0 to 5.08 cm (2 in.) Effective load was determined on a Mettler balance caplable of accuracy $\pm$ 0.01 mg.

Groove angles were photographed, on an ETEC scanning electron microscope operated by the Kansas State University Agricultural Experiment Station. Angle measurements of enlarged photographs were generally reproducable to $\pm$ 1°.

Table (3)
Composition of the
Alloy of Study*

(composition in weight-%)

Al	5.35
Sn	2.88
Fe	0.039
Mn	0.05
O	0.050
C	0.004
N	0.011
H	0.0092
Ti	-balance-

*Material Assay by
Aeromet Inc., Englewood, N.J.

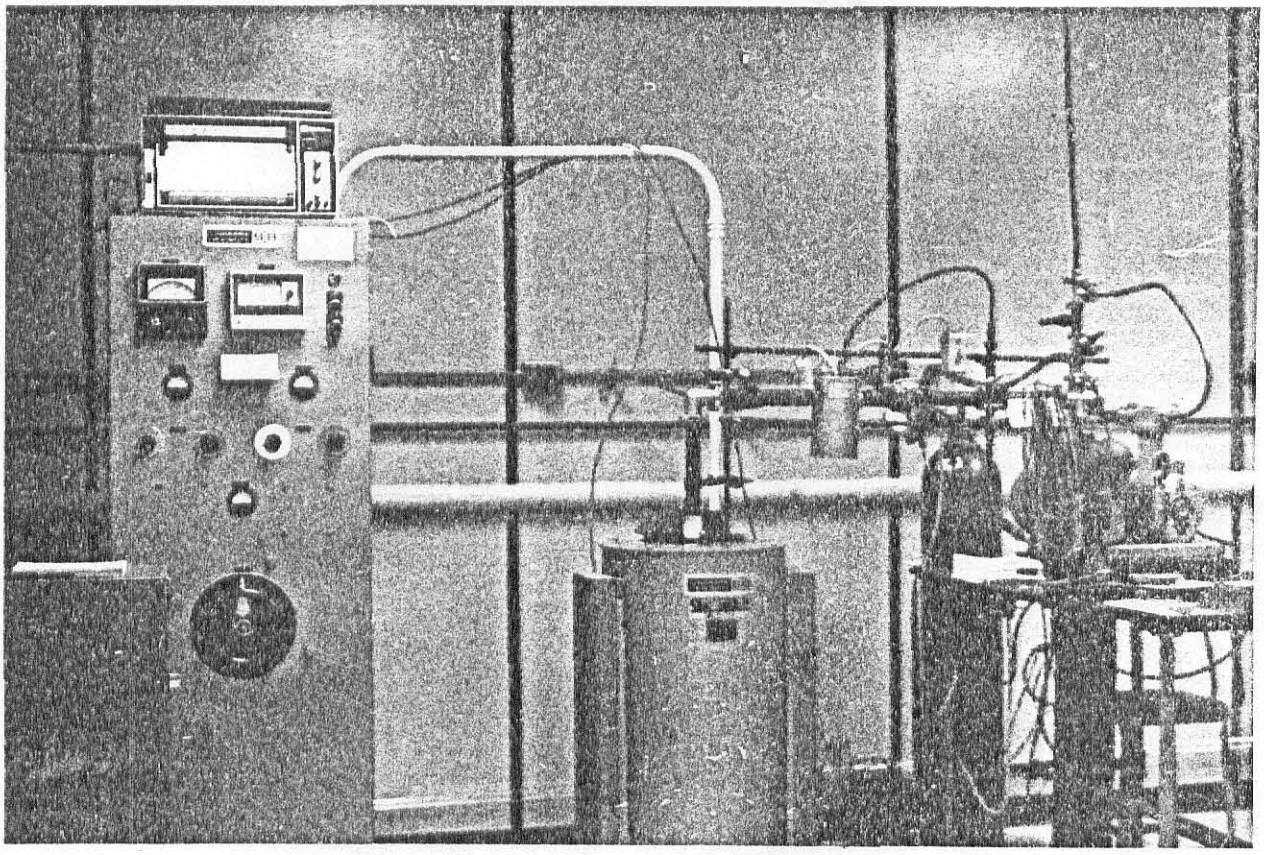

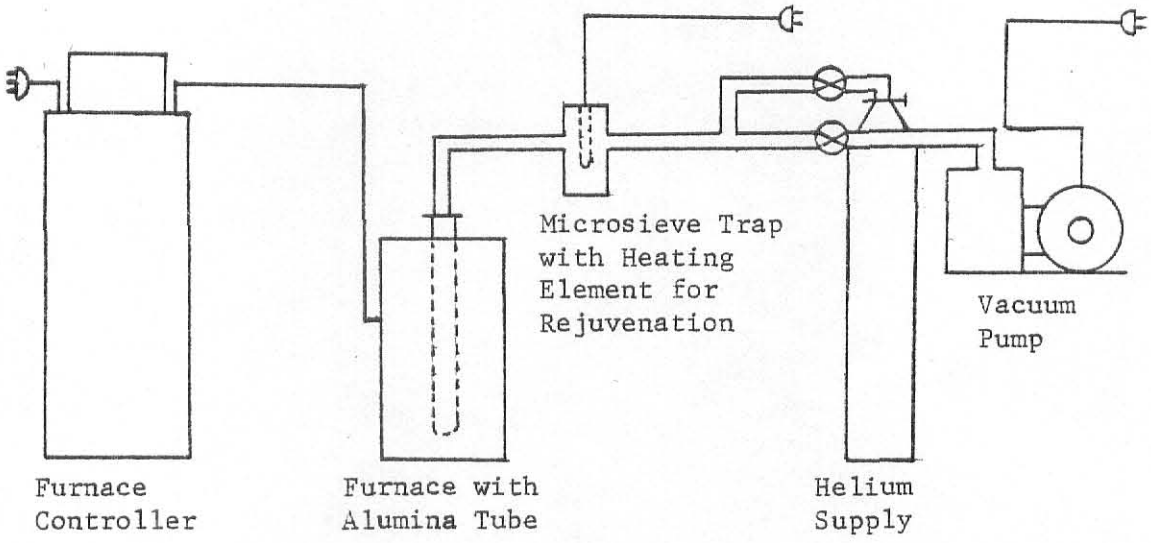

Figure (10)
Diagram of the Experimental Apparatus

IV. Results and Discussion

A. Surface and Grain Boundary Free Energies

The determination of the surface and grain boundary free energies of the titanium alloy Ti-5Aℓ-2.5Sn in purified helium atmosphere was performed at six different temperatures within the range 1377K to 1583K, or approximately 0.74 T_m to 0.85 T_m. Each sample consisted of a length of Ti-5Aℓ-2.5Sn wire with a loop at one end and a small titanium weight tied at the other. Small overhand knots were tied along the length of the wire to form several gauge lengths, typically seven or eight. Each sample was designated with a whole number (1,2,3, etc.) and each gauge length within was identified starting from the loop with a capital letter (A,B,C, etc.).

After sufficient anneal the samples displayed the desired bamboo structure as typified in Figure (11). The ridges and surface roughness shown were common to all samples and are the result of the hcp structure which occurs below approximately 1200K. A micrograph of higher magnification showing the surface structure is presented in Figure (12).

Results in the determination of interfacial energies are summarized in Table (4) and the temperature dependence is shown in Figure (13). A sample calculation detailing the means in which the data was analyzed is shown in Appendix I. The temperature dependence was found by subjecting the data in Table (4) to a linear regression between temperature and interfacial free energy. The data was best fit by the equations in SI units (J/m^2)

$$\lambda_s = -0.00203T + 4.57 \qquad (11)$$

$$\text{and } \lambda_{gb} = -0.000931T + 2.093 \qquad (12)$$

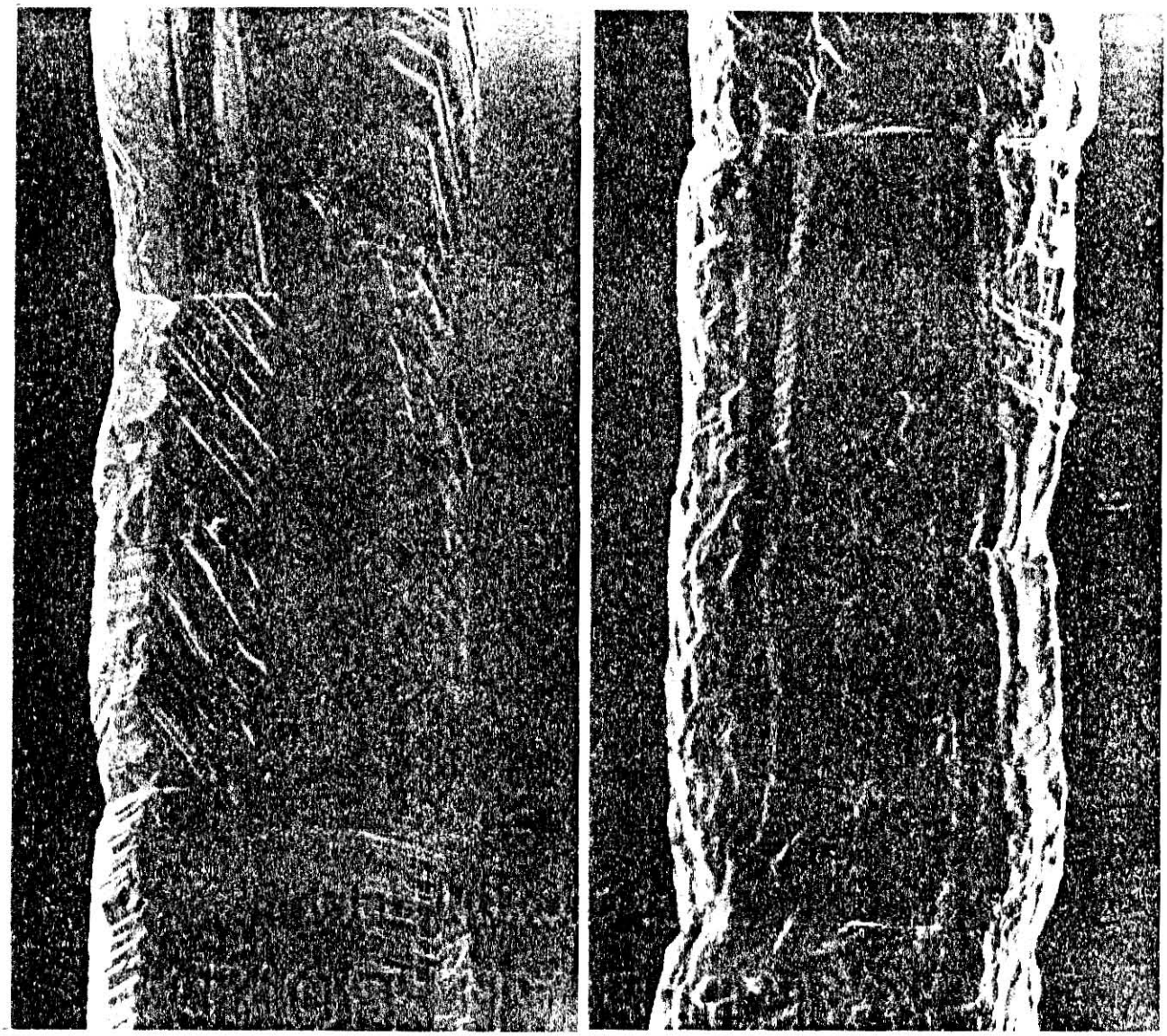

Figure (11)
Typical Micrographs of Fine Wires of Ti-5Aℓ-2.5Sn after Creep at Elevated Temperatures in He Atmosphere Showing Thermally Etched Grain Boundary Grooves.

(SEM Micrographs at 300X Magnification, Enlarged Slightly in Reproduction)

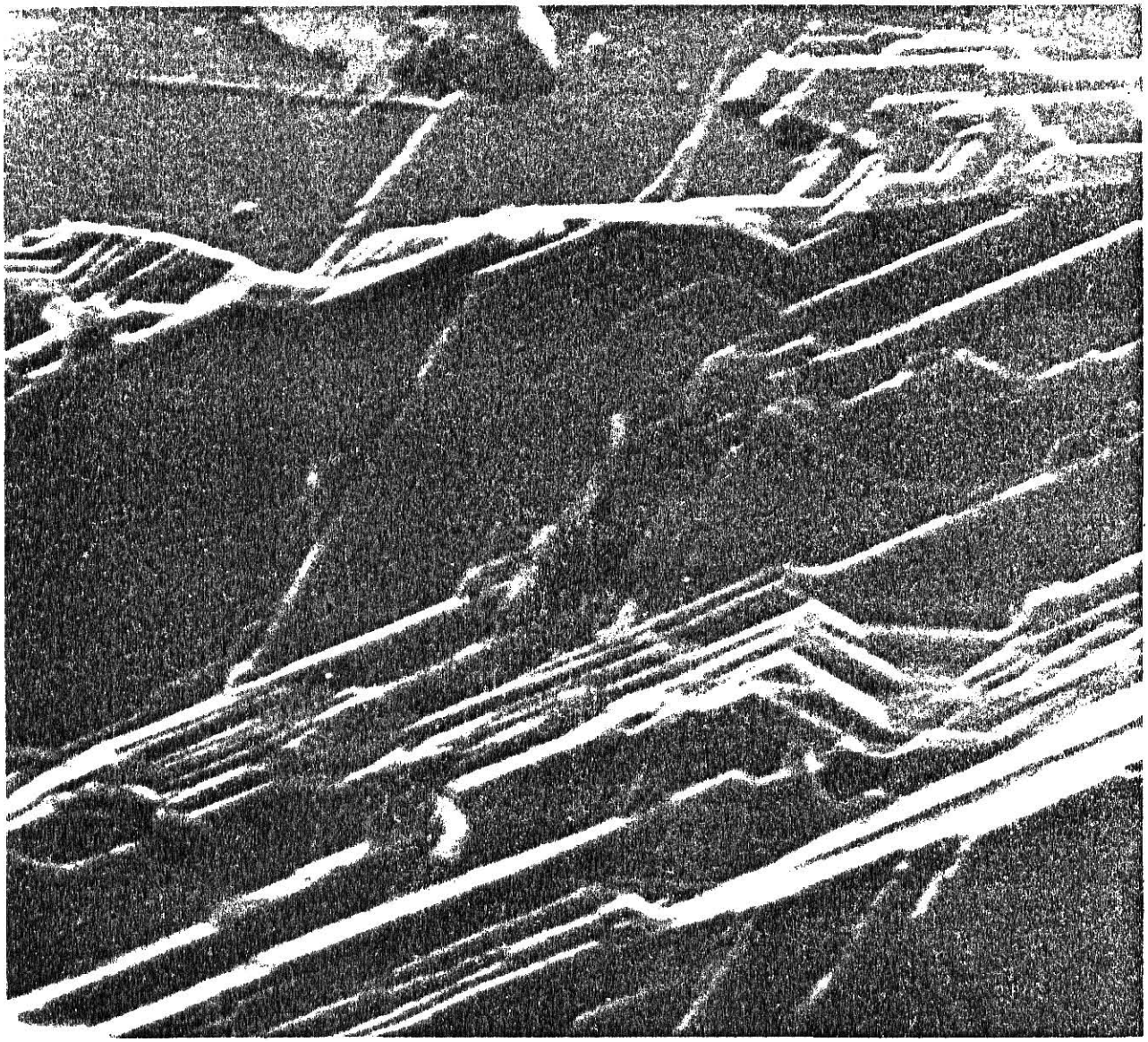

Figure (12)
Micrograph of the Surface of a
Ti-5Aℓ-2.5Sn Sample Crept at Elevated
Temperature in He Atmosphere.

(SEM Micrograph at 3000X Magnification,
Enlarged in Reproduction)

Table (4)
Summary of Results of Interfacial Free Energies
for Ti-5Aℓ-2.5Sn

Wire Radius = $5.08(10^{-5})$m
Median Grain Boundary Groove Angle = 153.5°(2.68 rad)

Sample Number	Temperature (K)	Creep Time (10^5 sec)	Grains/Meter ± Std. Error (m^{-1})	Balance Load ± Std. Error (10^{-4} N)	Surface Free Energy (J/m^2)	Grain Boundary Free Energy (J/m^2)
60	1377	3.456	3410±130	2.55±0.03	1.74	0.795
72	1413	3.24	3340±140	2.46±0.16	1.67	0.765
85	1455	3.024	3640±140	2.39±0.18	1.64	0.752
74	1508	3.024	3360±80	2.35±0.45	1.60	0.732
83	1563	2.592	3640± 200	2.04± 0.30	1.40	0.639
84	1563	2.592	3850± 110	2.02± 0.38	1.39	0.637
88	1583	2.232	3760± 130	1.87± 0.17	1.28	0.588

Figure (13)
The Temperature Dependence of the Surface and
Grain Boundary Free Energies of Ti-5Aℓ-2.5Sn

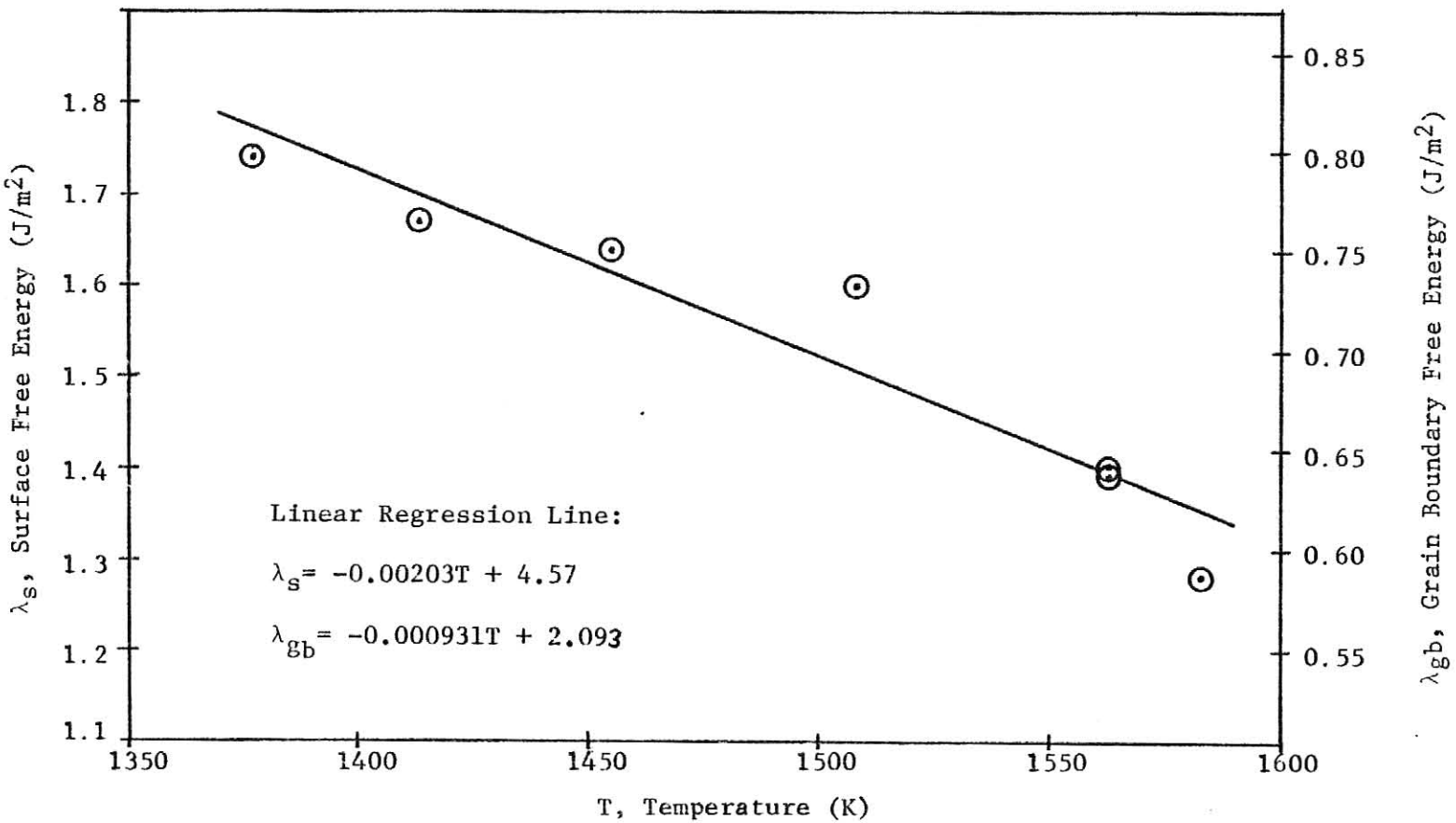

It is expected that points along the regression line better represent the truth than any individual data point. Further analysis reveals that the root-mean-square residual, the root-mean-square of the difference between the value of interfacial free energy between regression and individual data at the same temperature, is 0.018 J/m^2 or 1.2% of the overall mean (1.53 J/m^2 @ 1494K). Also, any additional single observation at the mean has a 0.9 probability of being within 0.12 J/m^2 (7.8%) of it.

Creep time varied between $3.456(10^5)$ sec (96 hrs.) at the lower temperatures to $2.232(10^5)$ sec (62 hrs.) at the higher temperatures. Because of a greater diffusion rate as temperature increases less time is required for a given amount creep.

The number of grains per meter between samples varied from 3340 grains/m to 3760 grains/m. Grain counts were taken over each gauge length in a sample. The standard error about the average within a sample was typically 4%.

The balance load was determined by the intercept of a plot of effective load versus strain for each sample. Statistical analysis allowed an estimation of the standard error of the determination in each case. Typically it was 10% of the balance load. Samples with error greater than 20% were not accepted. It is clear that the random error associated with the actual gauge length measurement, which is reproducable to within 0.05%, cannot account for this variability even though it is the nature of linear regression that the variance is greater for the estimate of an extrapolated point. Sources of error which could account for this variability are kinking or offsetting within a sample, both of which were periodically observed. Kinking is visualized as rotation of a grain about an axis thru the grain boundary. It occurs most frequently in lesser stressed and smaller diameter wires. Offsetting is a consequence of the viscousness of grain boundaries at elevated

temperature in which the boundary may flow or slide most often in a lateral direction. Offsetting occurs most frequently in higher stressed wires at higher temperatures and usually will have less bearing on results than would kinking. It is expected that the more these forms of deformation are found the greater the variability in the estimated balance load, especially if they occur unevenly across the sample. Also, it is possible in some cases that internal defects may have been present in the wire significant enough not to be eliminated by the first anneal or that sections of the wire may have been damaged in some fashion during handling despite care to avoid such an occurrence.

Several factors contributed to the difficulty of experiment. True gauge length measurements were required in order to obtain a reasonable balance load. Because of direct proportionality, any relative error in the balance load would be a minimum error in the surface free energy calculated from it. Considerable care was taken in handling the wires to avoid damage or surface contamination. Further precautions against surface contamination were taken during experiment as outlined previously in Chapter III.

Initially, effective loads on the order of 0.1 g were used, the same used by Roth and Suppayak[70] for Ti and Ti-6Al-4V. However, the balance loads determined, hence the interfacial free energies, were two to three times greater than reasonable. Reducing the effective loads to on the order of 0.05 g or less produced reasonable and reproducible results but created problems associated with such small loads as occasional wire entanglement during initial anneal or kinking, any of which could negate all or part of the usefulness of a sample. The surfaces of the greater loaded samples under high magnification appeared rough and sharply ridged, much more so than the following lesser loaded samples. It is possible that the higher loaded

samples were out of the range where creep was controlled by a Nabbaro-Herring mechanism.

Because there is no published data on the interfacial free energies of Ti-5Aℓ-2.5Sn direct comparison of the results of this study is not possible. However, useful comparisons can be made to data of other titanium alloys and to a number of empirical relations.

Although there are only limited comparisons that can be made to other experimental studies, there does exist a number of empirical relations between the surface free energy of metals and some bulk physical property. While these relations are by nature nonprecise, they do provide a means of comparison. Three such are shown in Figure (14). It should be noted that most of the data is for pure metals and that additional variation may be encountered when dealing with alloys.

L.E. Murr[24] demonstrated a relationship between surface free energy at 0.9 T_m (where T_m = melting point) and the modulus of elasticity in tension (Young's modulus) as seen in Figure (14a). Given that Young's modulus for Ti-5Aℓ-2.5Sn is $1.07(10^{11})$ N/m^2 ($15.5(10^6)$ psi, $10.8(10^3)$ kg/mm^2)[14] the surface free energy at 0.9 T_m would be predicted to be 1.65 J/m^2.

H. Jones[27] presented a relationship between the molar solid surface free energy and the heat of sublimation (H_{sv}) at T_m. It is, as shown in Figure (14b):

$$F_{sv} = KH_{sv} = (N)^{1/3}(U_m)^{2/3}\lambda_s \qquad (13)$$

where: K = a constant (0.15)
N = Avogadro's number ($6.023(10^{26})$ atoms/kmol)
U_m = molar volume of solid at T_m

The heat of sublimation for Ti-5Aℓ-2.5Sn was not available but was assumed

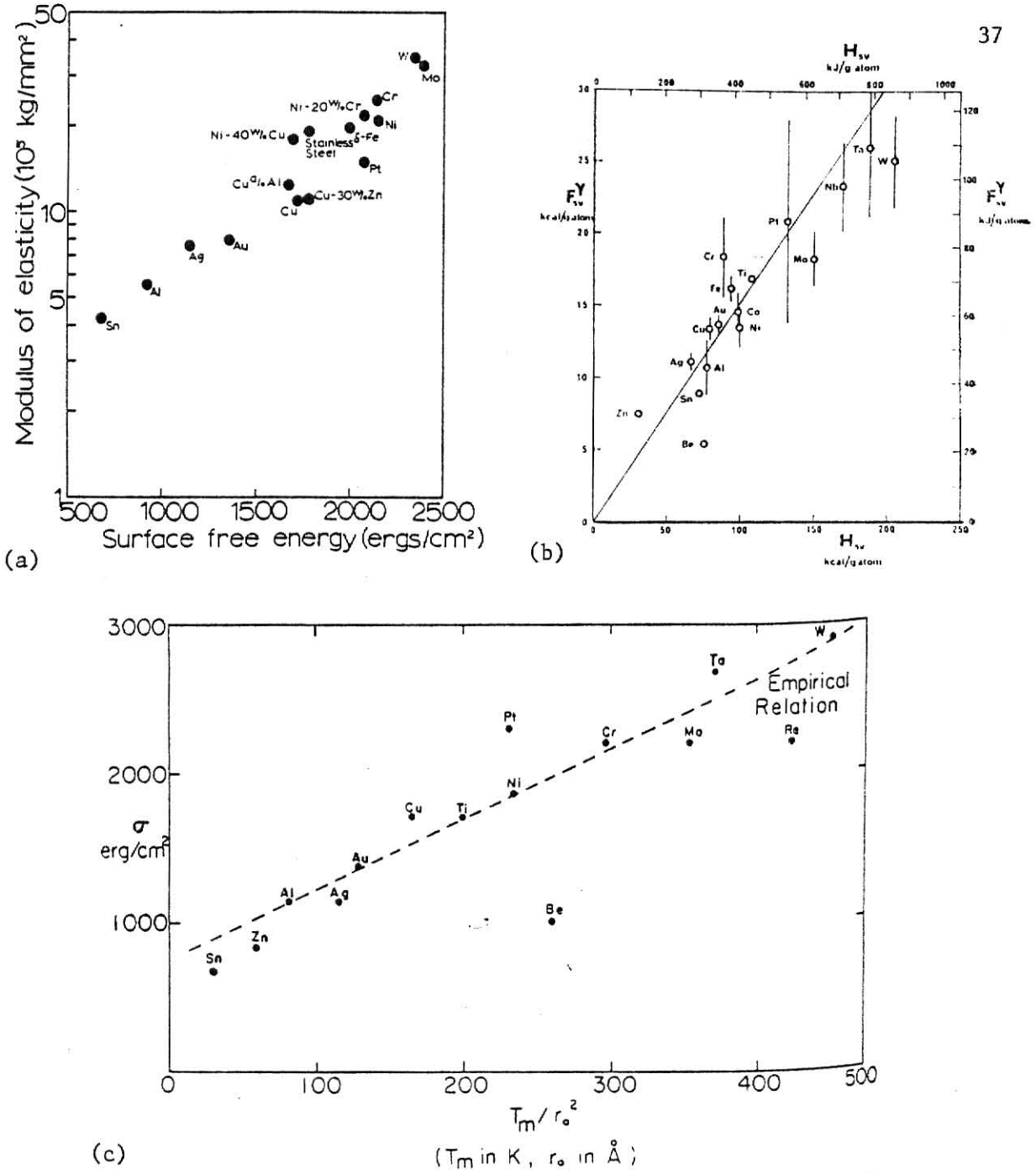

Figure (14)
Empirical Correlations to Surface Free Energy

(a) Surface Free Energy @ $0.9T_m$ versus Modulus of Elasticity in Tension (Youngs Modulus) (where: T_m=melting point). Reproduced from L. E. Murr[29].

(b) Molar Surface Free Energy versus Heat of Sublimation @ T_m. Reproduced from H. Jones[27].

(c) Surface Free Energy versus T_m/r_0^2 (where: r_0= nearest-neighbor separation). Reproduced from C. L. Reynolds, et. al.[72].

to be close to that for pure titanium, which is,[27] $H_{sv} = 4.5(10^8)$ J/kmol. Calculating as shown in Appendix II, $U_m = 0.011$ m^3/kmol. With this information and equation (13) the surface free energy is predicted to be 1.6 J/m^2 at the melting point.

Reynolds, Couchman, and Karasz[72] presented an empirical relationship with theoretical basis between surface free energy and the term T_m/r_o^2 (where r_o = nearest neighbor separation) as shown in Figure (14c):

$$\lambda_s = 0.76 + 4.77(10^{-23})\ T_m/r_o^2 \qquad (14)$$

This relationship is not corrected for temperature variation and represents a surface free energy near T_m. The nearest neighbor separation for Ti-5Aℓ-2.5Sn in the β-phase was not found, however, for β-Ti r_o = $2.9(10^{-10})$ m[73]. In the α-phase the lattice size tends to increase slightly with the addition of tin and decrease slightly with aluminum[74]. The same is expected in the β-phase. Thus, it would be expected that r_o would be nearly the same for both β-Ti and β-Ti-5Aℓ-2.5Sn. The melting temperature is taken as near the midpoint of the melting range, T_m = 1855K. With equation (14) the predicted surface free energy is 1.8 J/m^2.

Table (5) compares the surface free energy predicted by these empirical relations with results from this study. It can be seen that the empirical predictions are substantially higher than experimental but of the same order of magnitude. There are two possible explanations for this difference. First, the empirical relations were based on data mostly of pure metals. Alloys have tended to vary more from these relations. Secondly, it may be that extrapolation of experimental data does not apply well near the melting point. It could be concluded that the first is true since all the empirical

Table (5)
Comparison of Empirical and Experimental
Results for Ti-5Al-2.5Sn

Reference	Temperature	Surface Free Energy (J/m^2) Empirical	Experimental	Difference from Experiment (J/m^2)
Murr[29]	$0.9T_m$	1.65	1.18	0.47
Jones[27]	T_m	1.6	0.8	0.8
Reynolds, Couchman and Karasz[72]	near T_m	1.8	0.9	0.9

predictions of surface free energy are near or greater than the higher of the experimental results at the lower temperatures (1350K to 1500K). The second may or may not be true. As always, care should be taken when extrapolating data.

Figures (15) and (16) compare the results of this study with Roth and Suppayak[70] in their investigation with pure titanium and the alloy Ti-6Aℓ-4V. It is seen that the surface free energy of Ti-5Aℓ-2.5Sn is between 13% and 30% less than that for pure titanium while there is not as great a difference in the grain boundary free energies. Also, the temperature dependence was found to be greater for Ti-5Aℓ-2.5Sn. These differences can be explained in terms of temperature and compositional dependences of interfacial free energies.

The thermodynamic equation governing the temperature and compositional dependences of interfacial free energies was presented by Gibbs[63]:

$$d\lambda_i = -S_i dT - \sum_j \Gamma_j d\mu_j \qquad (15)$$

where: S_i = entropy of interface "i"

Γ_j = interfacial excess of component "j" in moles per interfacial area

μ_j = chemical potential of component "j"

The relation is easily derived from the Gibbs-Duhem equation applied to surfaces dropping the term $\Delta b dP$ (where Δb is the width of the interface and dP is the pressure differential) which is equivalent to neglecting PV terms for solids and liquids. Generally the width of the interface is no more than two monolayers.

Solute atoms in equilibrium in solid solution will sometimes concentrate at an interface such as a grain boundary or solid-vapor surface. This is

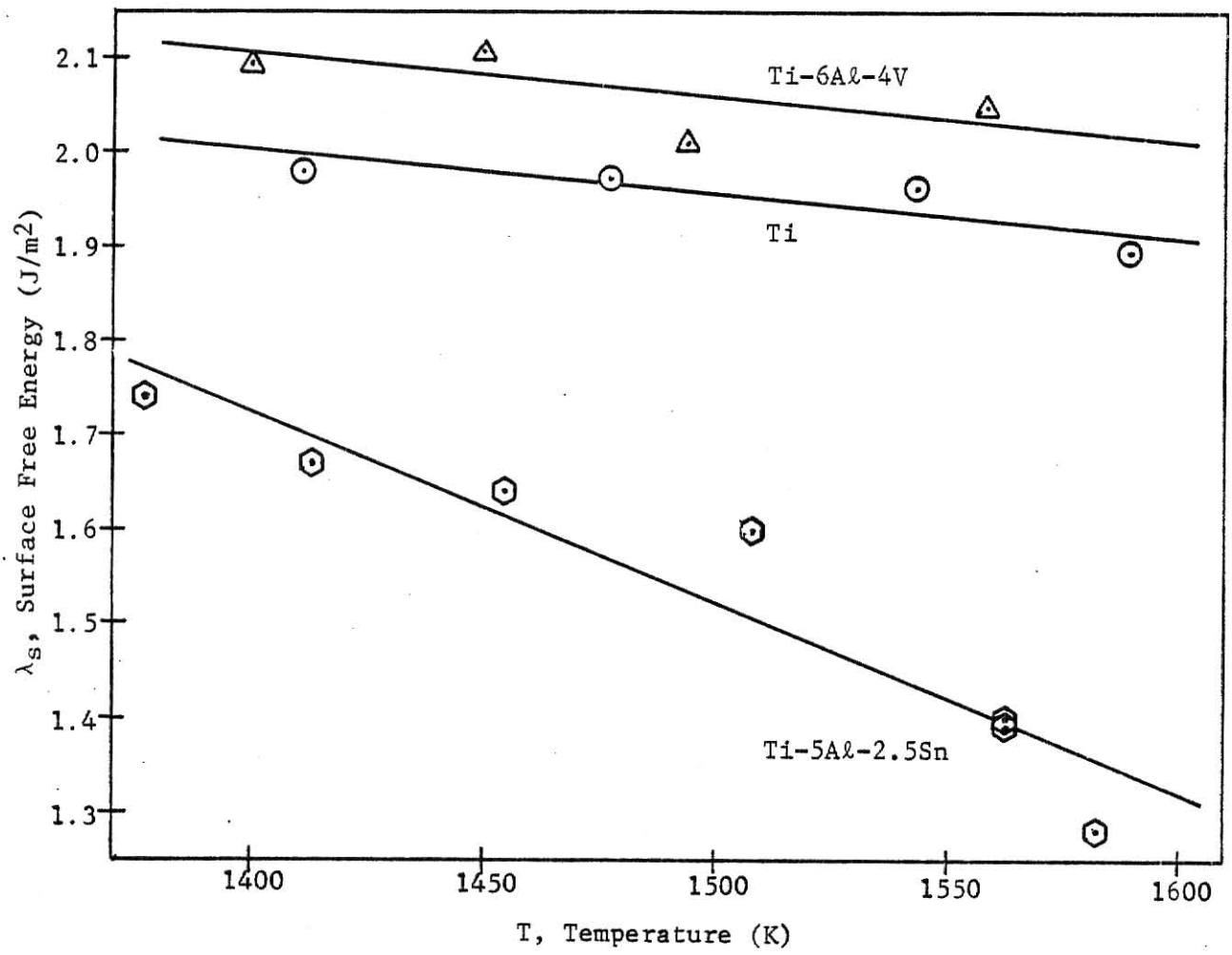

Figure (15)
Comparison of the Surface Free
Energies of Different Titanium Alloys

Alloy	Linear Fit	Reference
Ti-6Aℓ-4V	λ_s= -0.000443T +2.72	(70)
Ti	λ_s= -0.000435T +2.61	(70)
Ti-5Aℓ-2.5Sn	λ_s= -0.00203T +4.57	Present Work

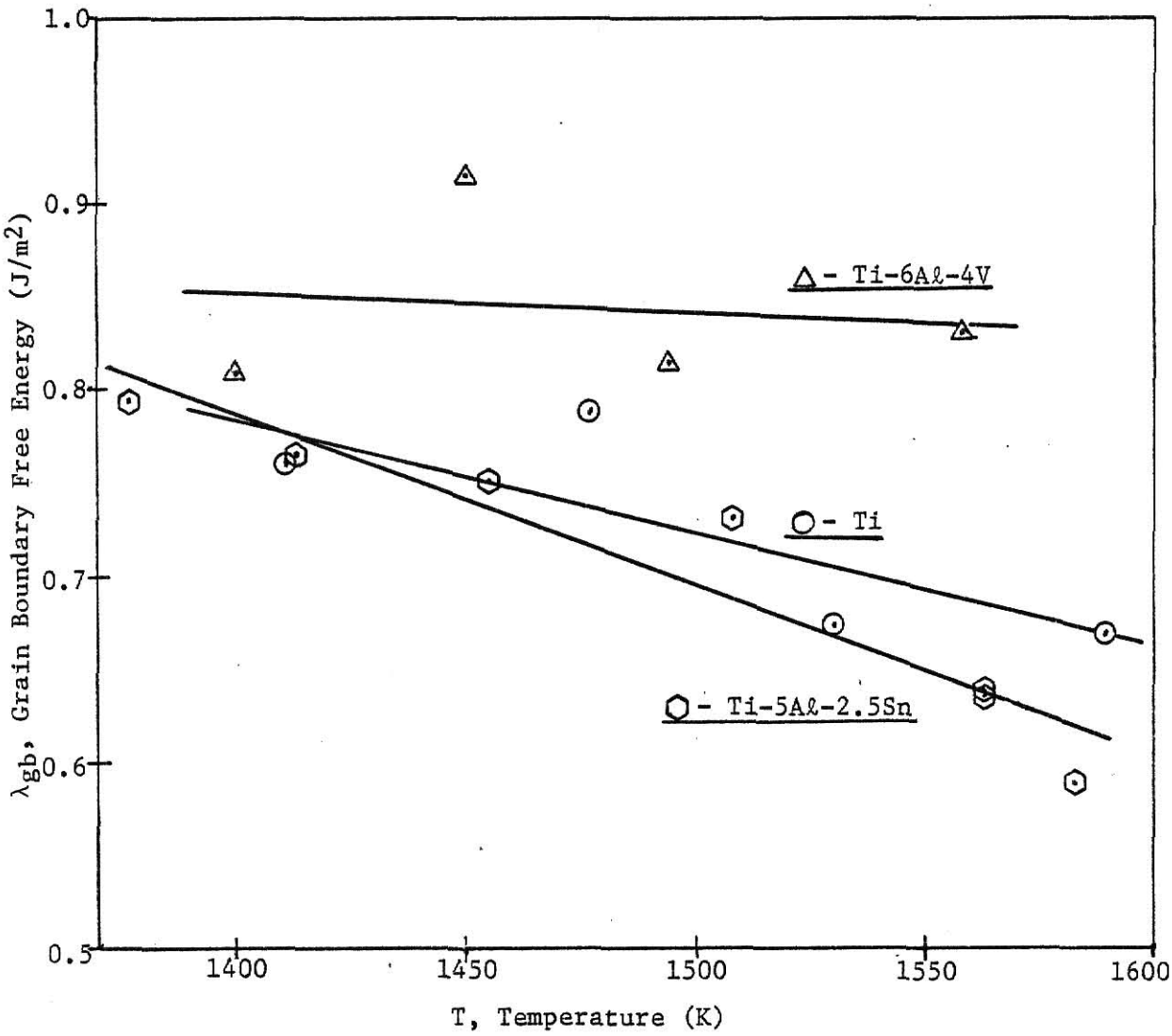

Figure (16)
Comparison of the Grain Boundary Free
Energies of Different Titanium Alloys

Alloy	Linear Fit	Reference
Ti-6Aℓ-4V	λ_{gb}= -0.00010T + 0.991	(70)
Ti	λ_{gb}= -0.00065T + 1.698	(70)
Ti-5Aℓ-2.5Sn	λ_{gb}= -0.000931T + 2.093	Present Work

termed equilibrium segregation. According to the thermodynamics presented by Gibbs, solute atoms which would decrease an interfacial free energy would tend to migrate toward that interface while solutes which increase it would tend to avoid the interface.

Equilibrium segregation can be examined by considering a solute atom occupying a site in the crystal lattice. This solute atom would be larger or smaller than the site normally occupied by an atom of solvent. In either case, lattice strain will occur. Such strains may contain a significant amount of energy and distortions in the lattice network can be quite considerable[75]. Due to discontinuities of the crystal, lattice sites near a solid-vapor surface or grain boundary are normally distorted and solute atoms may find themselves in sites more suited to their sizes. Thus the total lattice strain may be decreased by segregation of solutes to interfaces.

With this view it would be expected that tin would have greater effect on interfacial free energies in titanium than aluminum because of greater atomic size difference. As seen from Figures (15) and (16) a titanium alloy with approximately 6% aluminum and 4% vanadium (Ti-6Aℓ-4V) was found to have slightly greater surface and grain boundary free energies than pure titanium. The interfacial free energies found for Ti-5Aℓ-2.5Sn were less than that for pure titanium by a greater differential. With this and a segregation study on a beta titanium alloy in which it was found that vanadium had a tendency to deplete interfaces at elevated temperatures[76], it does appear that tin has the greater effect on the interfacial free energies of titanium, barring substantial differences in interfacial concentrations of interstitial impurities.

One measure of the magnitude of the segregation is the interfacial enrichment ratio, β_i:

$$\beta_i = x_i / x_b \qquad (16)$$

where: x_i = concentration of component at interface "i"
x_b = bulk concentration of component

Hondros and Seah[77] presented an empirical correlation between the grain boundary enrichment ratio and the atomic solid solubility of solute in solvent as shown in Figure (17). In β-titanium the atomic solid solubilities of tin and aluminum are approximately 11 at.% and 45 at.% respectively[74]. Thus, the grain boundary enrichment ratio of tin would expected to be between 10 and 100 and between 5 and 50 for aluminum. Generally, any interfacial enrichment greater than one would mean a reduction in the free energy of the interface. Such is the case when the surface and grain boundary free energies are compared between pure titanium and Ti-5Aℓ-2.5Sn.

Grain boundary enrichment can be observed in a metal sample thru energy dispersive x-ray analysis (EDX). An EDX system operates in conjunction with a scanning electron microscope (SEM) to provide a microatomic analysis. With this system energies of characteristic x-rays generated thru interaction of the SEM electron beam with the atoms in the spot analyzed are detected in a solid-state lithium-doped silicon electronic device. The x-rays produce a current in the detector from which a spectrum of x-ray counts within discrete energy levels can be obtained. Three specimens were selected from a group of tested samples then mounted, ground and etched. Microatomic analysis was done on each at several points both on and away from grain boundaries. Because EDX will give only relative atomic concentrations, analysis is done by comparison of one point to another. It was found that the grain boundaries contained a larger proportion of aluminum and tin than the bulk between boundaries, more so with tin than aluminum. Little, if any, difference

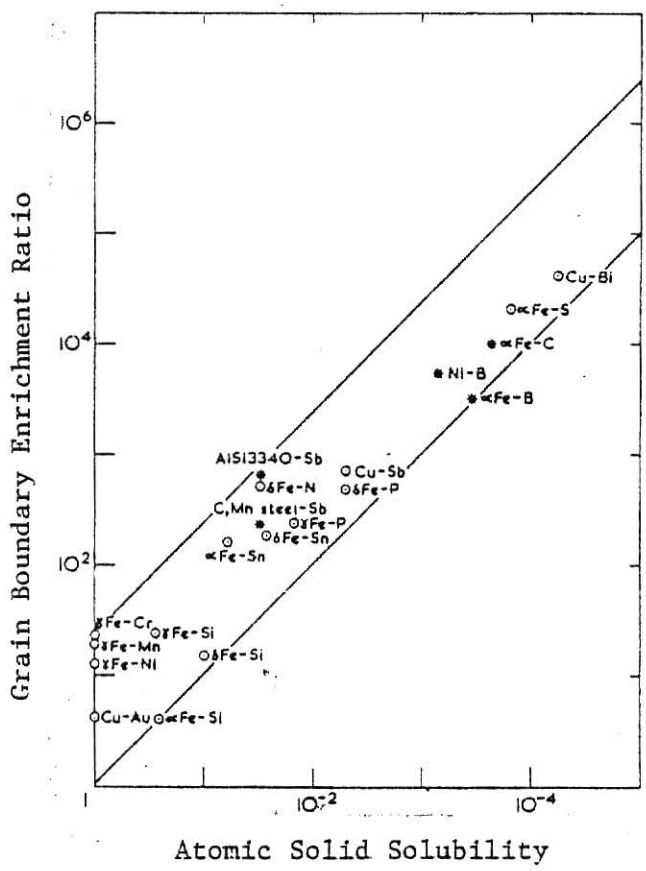

Figure (17)
Empirical Correlation Between Atomic Solid Solubility and Grain Boundary Enrichment Ratio.

From: E. D. Hondros and M. P. Seah, Int. Met. Rev., 22 (1977), 262.

existed in the atomic concentrations between different grain boundaries or between different points within the grains. Thus, grain boundary enrichment was observed for tin and aluminum in titanium.

Indirect evidence for equilibrium segregation exists in the magnitude of the grain boundary to surface free energy ratio determined from grain boundary groove angle measurements. Generally, for pure metals the ratio is near 1/3. For pure titanium it was found to be 0.37[70]. In this study the ratio for Ti-5Aℓ-2.5Sn was found to higher: 0.46. One explanation for this is that one or more of the solutes had a preference of segregation to the solid-vapor interface rather than the grain boundary. This behavior had been observed for tin in iron at 823K[78]. If this is the case the surface free energy would be reduced to a greater extent than the grain boundary free energy thus resulting in a higher grain boundary to surface free energy ratio.

Temperature dependence of surface or grain boundary free energy is described by a form of the Gibbs equation:

$$(d\lambda_i/dT)_V = -S_i - \sum_j \Gamma_j (d\mu_j/dT) \qquad (17)$$

For pure metals with no nonequilibrium concentrations of vacancies the last term on the right side of equation (17) would be zero and the temperature coefficient of the interfacial free energy would be equal to the negative of the interfacial entropy. Because entropy is always positive the temperature coefficient would not necessarily be negative. Generally for cubic pure metals $(d\lambda_s/dT) \simeq -4.5(10^{-4})$ J/m^{2}K[29].

For alloys the temperature coefficient is not necessarily negative, though generally it is. Only for strongly adsorbing interfaces or a large accumulation of contaminates has a temperature coefficient been found

positive[29]. Few temperature coefficients in alloys are found in the literature. For pure titanium and the alloy Ti-6Aℓ-4V the temperature coefficient of the surface free energy was found to be $-4.4(10^{-4})$ J/m^2K. For the grain boundary free energy the coefficients were $-6.5(10^{-4})$ J/m^2K and $-1.0(10^{-4})$ J/m^2K respectively[70]. In this study on Ti-5Aℓ-2.5Sn the temperature coefficients of the surface and grain boundary free energies were $-2.0(10^{-3})$ J/m^2K and $-9.3(10^{-4})$ J/m^2K respectively.

B. Anisotropy of Interfacial Free Energies

As previously mentioned, the interfacial energies determined in this study represent effective averages. A solid having an interfacial free energy that is isotropic would necessarily be amorphous. That crystalline materials are anisotropic is well known. Several studies have dealt with anisotropy of interfacial energies in metals[66-69]. Generally, grain boundary groove profiles are recorded by an electron microscope while crystalline orientatations are determined by analysis of back reflected x-rays. Such a procedure is laborious and beyond the scope of this study.

However, an indication of the extent of anisotropy of surface and grain boundary free energies in Ti-5Aℓ-2.5Sn can be seen in a histogram of grain boundary groove angle measurements as shown in Figure (18). Recalling equation (9),

$$\lambda_{gb}/\lambda_s = 2\cos(\Omega/2) \qquad (9)$$

where: Ω = grain boundary groove angle

it can be seen that the spread of the histogram is representative of the anisotropy of the ratio of grain boundary to surface free energies and not to either value specifically. McLean[66] and Hodgson and Mykura[67] have shown that the anisotropy of both are significant in copper and nickel, respectively.

It was found that the ratio λ_{gb}/λ_s was temperature independent within experimental error over the conditions encountered in this study. Generally, this conclusion can also be drawn from other similar experimental studies with limited temperature ranges. The median of all random grain boundary groove angle measurements was generally within 1° of the median of any particular sample. Moreover, the shape of the distribution was similar for all samples. Thus, the singular value $\Omega = 153.5^\circ$, or $\lambda_{gb}/\lambda_s = 0.458$, was used for all calculations.

Figure (18)
Histogram of Grain Boundary
Groove Angle Measurements

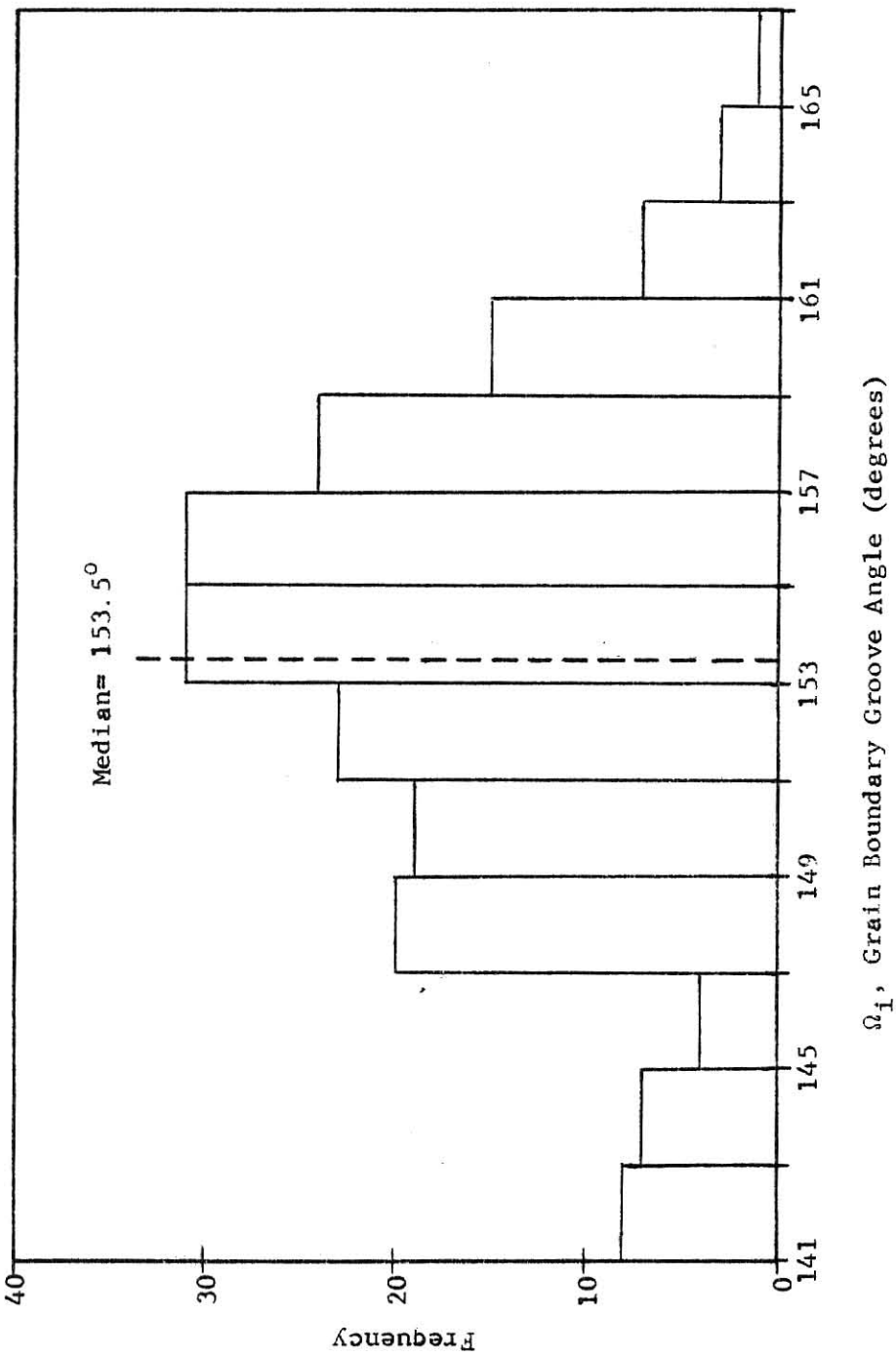

C. The Self-Diffusion Coefficient

During the course of this study sufficient data was taken to calculate self-diffusion coefficients and their temperature dependence for Ti-5Aℓ-2.5Sn using equation (3). A sample calculation detailing the means in which the data was manipulated is shown in Appendix I. Results of the determination of the self-diffusion coefficient are summarized in Table (6).

The value of the self-diffusion coefficient for each sample is the mean of values calculated from each gauge length. The standard errors in Table (6) for each coefficient, which average 27%, are an indication of the variability within each sample. Those with standard errors greater than 50% were not accepted. Because the criteria for accepting a data point was less stringent and because of the nature of analysis some samples which were not acceptable to estimate an interfacial free energy were accepted in this phase of study. Since the determination of an interfacial free energy requires a load intercept at zero creep, the balance load, greater accuracy would be obtained when the effective loads of each gauge length are near that intercept. This would entail that values of creep be near zero. In contrast, because the self-diffusion coefficient is proportional to creep, a higher value of creep is prefered to minimize relative error. Obtaining accurate interfacial free energies was given a higher priority in this study.

Generally, the temperature dependence of diffusion coefficients is best fitted to an Arrhenius type of expression. For Ti-5Aℓ-2.5Sn this expression is in SI units:

$$D = 5.7(10^{-6}) \exp[-1.82(10^{8})/RT] \quad (m^2/s) \qquad (18)$$

Table (6)
Summary of Results of Self-Diffusion
Coefficients for Ti-5Aℓ-2.5Sn

Sample Number	Temperature (K)	Creep Time (10^5 sec)	Self-Diffusion Coefficient ± Standard Error (10^{-13} m^2/sec)
59	1377	3.456	7.2±2.8
60	1377	3.456	6.8±2.7
68	1413	3.456	6.4±1.4
69	1413	3.672	12.7±5.4
71	1413	3.24	14.3±1.9
72	1413	3.24	11.1±4.3
85	1455	3.024	10.2±4.4
86	1455	3.024	11.4±4.3
73	1508	3.024	45±10
74	1508	3.024	39±5
81	1563	2.376	39±10
82	1563	2.376	52±9
83	1563	2.592	39±5
84	1563	2.592	44±8
87	1583	2.232	48±11
88	1583	2.232	55±11

Figure (18) presents this curve plotted with the data and compares it to results of other self-diffusion studies in titanium and titanium alloys.

There are two prevalent means of determining the self-diffusion coefficient in solid metals. The first is as described in this study and the second is thru the use of a radioactive tracer. In the second method a small amount of a radioactive diffusion species, for instance ^{44}Ti, is placed on a sample and allowed to diffuse at test temperature. Then the profile of radiotracer within the sample is determined using some sort of ionizing particle detector and a diffusion coefficient is calculated. The radiotracer technique is considered to be more reliable than creep tests in the determination of self-diffusion coefficients.

As seen in Figure (19) the self-diffusion coefficients in titanium metal and alloys determined thru zero creep are greater than those found thru radiotracer techniques. Table (7) presents the fitted expressions plotted in Figure (18). The exponential and pre-exponential factors for Ti-5Aℓ-2.5Sn are similar to those from the previous studies.

As previously mentioned, reasonable agreement between the two methods is expected when equation (4) is satisfied:

$$D_r t/(2r\bar{\ell}) \gtrsim 3 \qquad (4)$$

For the results of this study the left side of equation (4) was approximately equal to 3 for data at the lower temperatures up to 5 for data at the higher temperatures. Thus, it is expected that the results of this phase of this study are true within experimental error.

D. Recommendations for Future Study

The primary purpose of this study was to provide experimental values of the surface and grain boundary free energies and the self-diffusion coef-

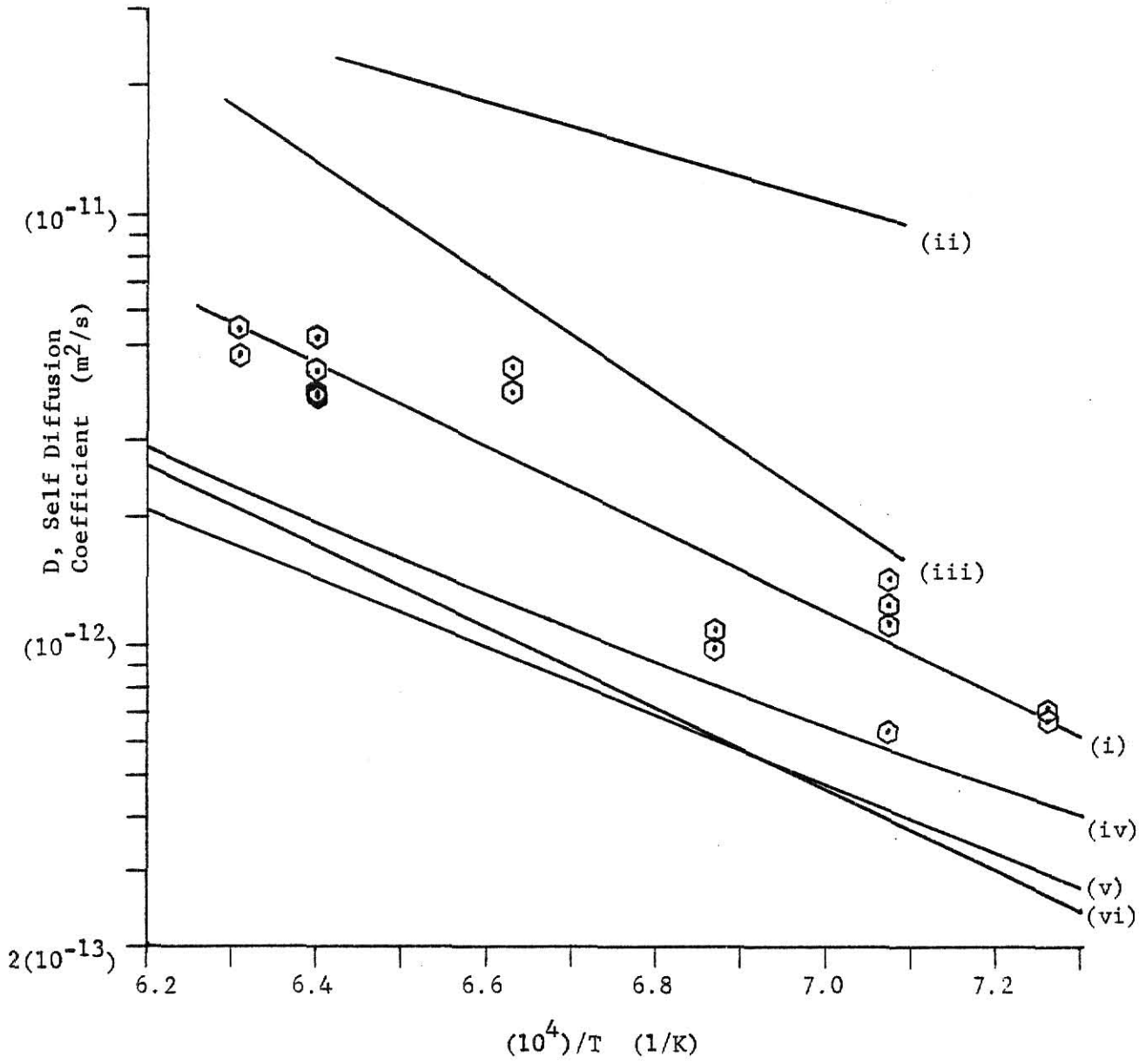

Figure (19)
The Temperature Dependence of Self Diffusion Coefficients in Titanium and Titanium Alloys

	Solvent	Method	Reference
(i)	Ti-5Aℓ-2.5Sn	Zero Creep	Present Work
(ii)	Ti-6Aℓ-4V	Zero Creep	(70)
(iii)	Ti	Zero Creep	(70)
(iv)	Ti	^{44}Ti Radiotracer	(79)
(v)	Ti	^{44}Ti Radiotracer	(80)
(vi)	Ti-10%V	^{44}Ti Radiotracer	(81)

Table (7)
Summary of the Temperature Dependence
of the Self-Diffusion Coefficient in
Titanium and Titanium Alloys

	Solvent	Fitted Self-Diffusion Coefficient (m^2/s)	Method	Reference
(i)	Ti-5Aℓ-2.5Sn	$D = 5.7(10^{-6})\exp(-1.82(10^8)/RT)$	Zero Creep	Present Work
(ii)*	Ti-6Aℓ-4V	$D = 8.9(10^{-8})\exp(-1.07(10^8)/RT)$	Zero Creep	Roth and Suppayak[70]
(iii)*	Ti	$D = 3.6(10^{-3})\exp(-2.52(10^8)/RT)$	Zero Creep	Roth and Suppayak[70]
(iv)	Ti	$D = 3.58(10^{-8})\exp(-1.31(10^8)/RT) + 1.09(10^{-4})\exp(-2.51(10^8)/RT)$	^{44}Ti Radiotracer	Murdock, Lundy and Stansbury[79]
(v)	Ti	$D = 1.9(10^{-7})\exp(-1.53(10^8)/RT)$	^{44}Ti Radiotracer	DeReca and Libanati[80]
(vi)*	Ti-10%V	$D = 2.0(10^{-6})\exp(-1.81(10^8)/RT)$	^{44}Ti Radiotracer	Murdock and McHargue[81]

*Arrhenius expression fitted to published data by author of present work. Only data in the temperature range used in the present work is considered.

ficient at elevated temperatures for the titanium alloy Ti-5Aℓ-2.5Sn and to compare the results to previous work whenever possible. In that by all indications titanium alloys will be increasingly more important in the future, similar studies with other titanium alloys are recommended. Useful empirical or thermodynamic based relations could result from these and detailed segregation studies. In this study the self-diffusion coefficient is subject to a good deal of variability. A more confident coefficient can be obtained from a radiotracer diffusion study.

Development of a method of in-situ gauge length measurement would be useful in this type of research. An x-ray source and photographic plate could be utilized to record gauge lengths while the sample remains within the furnace at test temperature. This would eliminate the need to cool the samples before measurement. Also, many measurements could be taken over the course of the test. Thus, more accurate and confident creep rates could be determined, the dynamics of the creep anneal could be observed and time could be saved.

V. Conclusions

The method of zero creep in fine wires was used to investigate the surface and grain boundary free energies and the self-diffusion coeffecient in the titanium alloy Ti-5Aℓ-2.5Sn. The experiment was preformed in a purified helium atmosphere at six different temperatures within the range 1377K to 1583K. It was found:

(1) The surface free energy of Ti-5Aℓ-2.5Sn ranged from 1.28 J/m^2 to 1.74 J/m^2 and was best fit by the linear regression

$$\lambda_s = -0.00203T + 4.57 \qquad (J/m^2)$$

The grain boundary free energy ranged from 0.588 J/m^2 to 0.795 J/m^2 and was best fit by the regression line

$$\lambda_{gb} = -0.000931T + 2.093 \qquad (J/m^2)$$

For these linear regressions the 90% confident prediction interval at the overall mean was 7.8% of that mean. The interfacial free energies of Ti-5Aℓ-2.5Sn where less than those determined in a previous study for Ti and Ti-6Aℓ-4V. These differences were explained thru equilibrium segregation of solutes to the interfaces. A relatively high grain boundary to surface free energy ratio, $\lambda_{gb}/\lambda_s = 0.46$, seemed to indicate a segregational preference for the surface.

(2) The self-diffusion coefficient for Ti-5Aℓ-2.5Sn under a Nabarro-Herring mechanism of deformation was best fit by the Arrhenius expression in SI units

$$D = 5.7(10^{-6})\exp[-1.82(10^8)/RT] \qquad (m^2/s)$$

Comparisons to literature show reasonable agreement.

REFERENCES

(1) ASM News, September, 1980.

(2) G. T. Hahn, M. F. Kanninen and A. R. Rosenfield, Annu. Rev. Mater. Sci., 2 (1972) 381.

(3) A. Kelly, "Strong Solids", Clarendon Press, Oxford (1973).

(4) A. J. Shaler, Seminar on Kinetics of Sintering., AIME Met. Tech., December, 1948.

(5) A. T. Kuhn, "Industrial Electrochemical Processes", Elsevier, London (1971), p. 334.

(6) S. Roy, V. Sivan, V. Balasubramaniyan and B. A. Shenoi, Surface Tech., 7 (1978), 239.

(7) G. L. C. Bailey and H. C. Watkins, Proc. Physical Society of London (B), 63 (1950), 350.

(8) M. P. Seah, Surface Science, 80 (1979), 8.

(9) C. S. Smith, AIME Met. Tech., June 1948, TP 2387.

(10) P. Suppayak, "The Surface and Grain Boundary Free Energies of Pure Titanium and the Titanium Alloy Ti-6Aℓ-4V", Masters Thesis, Kansas State University (1977).

(11) F. R. N. Nabarro, "Report on Conference on Strength of Solids", Physical Society, London (1948), p. 75.

(12) C. Herring, J. Appl. Phys., 21 (1950), 459.

(13) A. D. McQuillan and W. K. McQuillan, "Titanium", Butterworths Publications, London (1956), pp. 337-46, 402-27.

(14) "Titanium Alloys Handbook", Air Force Materials Laboratory, MCIC-HB-02 (1972), Section 1.

(15) W. L. Finlay, R. I. Jaffee, R. W. Parcel and R. C. Durstein, J. Metals, 6 (1954), 25.

(16) "Aerospace Structural Metals Handbook", Air Force Materials Laboratory, MCIC-HB-02 (1972), Sec. 3706.

(17) C. J. Echer, J. E. Cooney and A. J. Kish, Metals Eng. Q., 7 (1978), 58.

(18) A. Kh. Breger and A. A. Zhukhoritskii, Zh. Fiz. Khim., 20 (1946), 355.

(19) R. Stratton, Phil. Mag., 44 (1953), 519.

(20) S. N. Zadumkin, Dokl. Akad. Nauk SSSR, 101 (1955), 507.

(21) A. S. Skapski, Acta. Met., 4 (1956), 576.

(22) S. N. Zadumkin, Fiz. Metal Metalloved, 11 (1961), 331.

(23) V. K. Semenchenko, "Surface Phenomena in Metals and Alloys", Pergamon Press, New York (1962).

(24) S. N. Zadumkin, Institute for Powder Metallurgy and Special Alloys, Izd. Akad. Nauk, Ukr. SSR, Kiev (1963), p. 7.

(25) Y. S. Avraamov and A. G. Gvozdev, Fiz. Metal Metalloved., 23 (1967), 405.

(26) S. N. Zadumkin, A. I. Temrokov, I. G. Shebzukhora and I. M. Aliev, Institute for Material Science Problems, Izd. Naukova Dumka, Kiev (1968), p. 9.

(27) H. Jones, Metal Sci. J., 5 (1971), 15.

(28) W. Missol, Phys. Stat. Sol. B, 58 (1973), 767.

(29) L. E. Murr, "Interfacial Phenomena in Metals and Alloys", Addison-Wesley, Reading, Mass. (1975), pp. 122-38.

(30) E. Zaremba, Solid State Commun., 23 (1977), 347.

(31) R. Chang, Scripta Met., 14 (1980), 779.

(32) J. Frenkel, Z. Phys., 51 (1928), 232.

(33) J. Bardeen, Phys. Rev., 49 (1936), 653.

(34) P. Hohenberg and W. Kohn, Phys. Rev. B, 136 (1964), 864.

(35) W. Kohn and L. J. Sham, Phys. Rev. A, 140 (1956), 1133.

(36) J. R. Smith, Phys. Rev., 181 (1969), 522.

(37) N. D. Lang and W. Kohn, Phys. Rev. B, 1 (1970), 4555.

(38) M. D. Rouhani and R. Schattler, Surface Sci., 38 (1973), 499.

(39) R. Monnier and J. P. Perdew, Phys. Rev. B, 17 (1978), 2595.

(40) C. C. Pei, Phys. Rev. B, 18 (1978), 2583.

(41) L. E. Murr, "Interfacial Phenomena in Metals and Alloys", Addison-Wesley, Reading, Mass. (1975) p. 116.

(42) M. C. Inman and H. R. Tipler, Met. Rev., 8 (1963), 105.

(43) H. Udin, "Metal Interfaces", Am. Soc. Metals (1952), p. 114.

(44) J. B. Hess, "Metal Interfaces", Am. Soc. Metals (1952), p. 134.

(45) J. C. Fisher and C. G. Dunn, "Imperfections in Nearly Perfect Crystals", Wiley, New York (1952), p. 317.

(46) I. Sawai and M. Nishida, Z. Anorg. Allg. Chem., 190 (1930), 375.

(47) G. Tamman and W. Boehme, Ann. Phys., 12 (1932), 820.

(48) H. Udin, A. J. Shaler and J. Wulff, Trans. AIME, 185 (1949), 186.

(49) A. Udin, Trans. AIME, 191 (1951), 63.

(50) A. L. Pranatis and G. M. Pound, Trans. AIME, 203 (1955), 664.

(51) E. D. Hondros, Proc. Roy. Soc. A, 286 (1965), 479.

(52) J. J. Bikerman, Phys. Status Solidi, 10 (1965), 3.

(53) J. J. Bikerman, "Physical Surfaces", Academic Press, New York (1970), p. 207.

(54) J. J. Bikerman, Mat. Sci. Engg., 20 (1975), 293.

(55) R. Shuttleworth, Proc. Phys. Soc. (London) A, 63 (1950), 444.

(56) F. V. Nolfi and C. A. Johnson, Acta Met., 20 (1972), 769.

(57) B. Chalmers, R. King and R. Shuttleworth, Proc. Roy. Soc. A, 193 (1948), 465.

(58) M. C. Inman, D. McLean and H. R. Tipler, Proc. Roy. Soc. (London) A, 273 (1963), 538.

(59) B. C. Allan, Trans. AIME, 236, (1966), 903.

(60) A. P. Greenough, Phil. Mag., 3 (1958), 1032.

(61) H. Jones, Mat. Sci. Eng., 4 (1969), 106.

(62) C. S. Smith, Trans. AIME, 175 (1948), 15.

(63) J. W. Gibbs, "The Scientific Papers of J. Willard Gibbs", Vol. I, Dover Publications, New York (1961).

(64) P. Curie, Z. Kristallogr., 12 (1897), 651.

(65) G. Wulff, Z. Kristallogr., 34 (1901), 449.

(66) M. McLean, J. of Mat. Sci., 8 (1973), 571.

(67) B. K. Hodgson and H. Mykura, J. of Mat. Sci., 8 (1973), 565.

(68) M. McLean and B. Gale, Phil. Mag., 20 (1969), 1033.

(69) O. K. Riegger and L. H. Van Vlack, Trans. AIME, 218 (1960), 933.

(70) T. A. Roth and P. Suppayak, Mat. Sci. Eng., 35 (1978), 187.

(71) L. E. Murr, O. T. Inal and G. I. Wong, "Electron Microscopy and Structure of Materials", University of California Press, Berkeley (1972), pp. 417-26.

(72) C. L. Reynolds, P. R. Couchman and F. E. Karasz, Phil. Mag., 34 (1976), 659.

(73) W. B. Pearson, "Handbook of Lattice Spacings and Structures of Metals and Alloys", Pergomon Press, Oxford (1967), p. 90.

(74) A. D. McQuillan and M. K. McQuillan, "Titanium", Butterworths Publications, London (1956), pp. 172-7, 265-8.

(75) D. McLean, "Grain Boundaries in Metals", Oxford University Press, London (1957), pp. 116-50.

(76) H. J. Rack, Metall. Trans. A, 6 (1975), 947.

(77) E. D. Hondros and M. P. Seah, Int. Met. Rev., 22 (1977), 262.

(78) C. Lea and M. P. Seah, Scr. Metall., 9 (1975), 583.

(79) J. F. Murdock, T. S. Lundy and E. E. Stansbury, Acta Metall., 12 (1964), 1033.

(80) N. E. W. DeReca and C. M. Libanati, Acta Metall., 16 (1968), 1297.

(81) J. F. Murdock and C. F. McHargue, Acta Metall., 16 (1968), 493.

Appendix I: Sample Calculations

The data of sample 83 is used for this example. Table (A1) contains the raw data for this sample. For each gauge length the amount of creep was calculated using equation (2):

$$\varepsilon = (\ell-\ell_o)/\ell_o \qquad (2)$$

The number of grains per meter was determined and the effective load, W, was converted from mass to force, f, for each gauge length. The results of these manipulations are shown in Table (A2). To find the balance load, f_0, a plot of creep versus effective load was prepared and a least squares linear regression was applied as shown in Figure (A1). The balance load was found to be $2.04(10^{-4})$N with a standard error of $0.30(10^{-4})$N.

With the knowledge that the median grain boundary groove angle, Ω, is 153.5°, enough information is available to calculate interfacial free energies thru the use of equations (9) and (10):

$$\lambda_{gb} = 2\lambda_s \cos(\Omega/2) \qquad (9)$$

$$\lambda_s = \frac{f_0}{\pi r\,[1-2r(n/\ell)\cos(\Omega/2)]} \qquad (10)$$

For sample 83 it was found that $\lambda_s = 1.40$ J/m^2 and $\lambda_{gb} = 0.639$ J/m^2.

To calculate a self-diffusion coefficient, equation (3) is used:

$$D = (2\varepsilon\bar{\ell}rRT)/(t\beta U\sigma) \qquad (3)$$

The mean grain length, $\bar{\ell}$, is simply the inverse of (n/ℓ) and the effective stress on a gauge length, σ, was found by dividing the effective load, f, by the cross sectional area of the wire. The volume per mole of atoms, U, is estimated to be equal to 0.0109 m^3/kmol by a method outlined in Appendix II.

Table (A1)
Raw Data for Sample 83

Radius: $r = 5.08(10^{-5})$m
Temperature: T= 1563K
Creep Time: $t = 2.592(10^{5})$sec = 72hr

Gauge Length	ℓ_o (in)	ℓ (in)	n	W (mg)
A	1.2431	1.2692	118	40.64
B	1.2832	1.3072	110	39.21
C	1.2732	1.2960	128	37.88
D	1.4152	1.4342	133	36.46
E	0.8403	0.8524	75	35.11
F	0.9912	1.0056	97	33.99
G	0.9880	1.0017	94	32.86
H	0.9257	0.9379	-	31.81

Surface Condition: acceptable

Table (A2)
Results of Raw Data Manipulation
for Sample 83

Gauge Length	ε	n/ℓ (m^{-1})	f (10^{-4}N)
A	0.02100	3660	3.985
B	0.01870	3310	3.845
C	0.01791	3890	3.715
D	0.01343	3650	3.575
E	0.01440	3460	3.443
F	0.01453	3800	3.333
G	0.01387	3690	3.222
H	0.01318	-	3.119

Mean $(n/\ell) = 3640\ m^{-1}$
Std. Error= $200\ m^{-1}$

Figure (A1)
Determination of the Balance
Load, f_0, for Sample 83

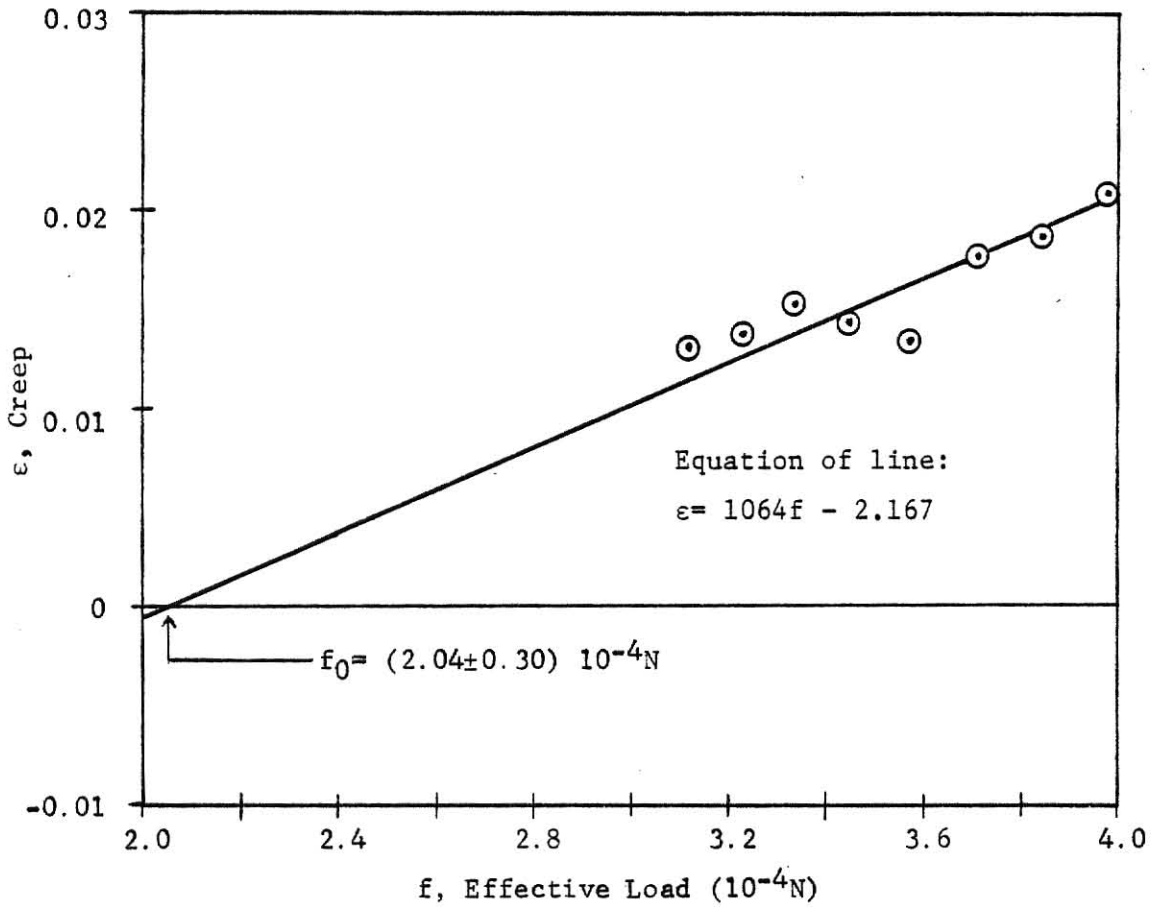

The results of calculations are shown in Table (A3). For sample 83 the the self-diffusion coefficient was found to be equal to $3.9(10^{-12})$ m^2/s with a standard error, which represents the variation among the gauge lengths, equal to $0.5(10^{-12})$ m^2/s.

Table (A3)
Calculations Towards a Self-Diffusion
Coefficient for Sample 83

$r = 5.08(10^{-5})$ m
$R = 8314$ J/K·kmol
$T = 1563$ K
$t = 2.592(10^{5})$ sec
$\beta = 12$
$U = 0.0109$ m^3/kmol

Gauge Length	$\bar{\ell}$ $(10^{-4}m)$	ε	σ $(10^{4}N/m^2)$	D $(10^{-12}m^2/s)$
A	2.73	0.02100	4.92	4.54
B	3.02	0.01870	4.74	4.64
C	2.57	0.01791	4.58	3.91
D	2.74	0.01343	4.41	3.25
E	2.89	0.01440	4.25	3.81
F	2.63	0.01453	4.11	3.62
G	2.71	0.01387	3.98	3.68

Mean Self-diffusion Coefficient: $D = 3.9(10^{-12})$ m^2/s
Standard Error: $0.5(10^{-12})$ m^2/s

Appendix II: Calculation of Molar Volume, U

Although molar volume is generally not published at elevated temperatures for metals it can be calculated using an appropriate expansion coefficient:

$$\Delta U/U = \alpha_v \Delta T \qquad \text{(A1)}$$

where: α_v = volume expansion coefficient which for virtually all materials $\alpha_v = 3\alpha_l$, three times the linear coefficient of expansion.

For Ti-5Aℓ-2.5Sn from room temperature to near the melting point, $\alpha_l = 1.1(10^{-5})$ $1/K$[16]. Specific volume is $\hat{V} = 2.24(10^{-4})$ m^3/kg[16] at room temperature. Given the composition of the alloy of study in Table (3), the same in mole fractions would be 0.896 Ti, 0.093 Aℓ and 0.011 Sn ignoring all other components. With this, the molecular weight would be 46.7 kg/kmol and the molar volume at room temperature would be $U_{RT} = 0.0105$ $m^3/kmol$

Combining the above information:

$$\Delta U = 3.456(10^{-7})\ (T - 298K)\ (m^3/kmol) \qquad \text{(A2)}$$

$$U_T = U_{RT} + \Delta U \qquad \text{(A3)}$$

Appendix III: Nomenclature

A_i : area of interface "i"

Δb : width of interface

D : self-diffusion coefficient

D_r : radiotracer estimate of the self-diffusion coefficient

f : static force due to gravity

f_0 : balance load

F_{sv} : molar solid surface free energy

g : acceleration due to gravity

H_{sv} : heat of sublimation at melting point

K : a constant, = 0.15

ℓ : final gauge length or overall wire length

ℓ_0 : initial gauge length

$\bar{\ell}$: mean grain length

n : Avogadro's number

P : pressure

r : wire radius

R : gas constant

r_0 : nearest neighbor separation

S_i : entropy of interface "i"

t : time of creep

T : absolute temperature

U : molar volume

V : volume

W_0 : balance mass

x_i : concentration of component at interface "i"

x_b : bulk concentration of component

α_l : linear coefficient of expansion

α_v : volume expansion coefficient

β : a constant, $\simeq 12$ when $\bar{\ell} \geq 2r$

β_i : enrichment ratio at interface "i"

Γ_j : interfacial excess of component "j"

σ : stress on the wire

σ_i : tension of interface "i"

ε : strain or creep

λ : free energy of interface "i"

μ_j : chemical potential of component "j"

Ω : grain boundary groove angle

Subscripts

s : surface

gb : grain boundary

m : at melting temperature

RT : at room temperature

THE SURFACE AND GRAIN BOUNDARY FREE ENERGIES AND THE SELF-DIFFUSION COEFFICIENT OF THE TITANIUM ALLOY Ti-5Aℓ-2.5Sn

by

WILLIAM DALE HENNING

B.S., Kansas State University, 1979

AN ABSTRACT OF A MASTER'S THESIS

submitted in partial fulfillment of the

requirements for the degree

MASTER OF SCIENCE

Department of Chemical Engineering

KANSAS STATE UNIVERSITY
Manhattan, Kansas

1981

Abstract

Using the method of zero creep in fine wires, previously undetermined absolute values of the surface and grain boundary free energies, λ_s and λ_{gb}, were determined in the temperature range 1377 to 1583K in an inert helium atmosphere for the titanium alloy Ti-5Aℓ-2.5Sn, an important alloy in aerospace and cryogenic industries. The creep of the fine wires in this study was assumed to be linearly controlled by a Nabarro-Herring mechanism.

The surface and grain boundary free energies were best fit by the following linear functions of temperature, T (K):

$$\lambda_s = -0.00203T + 4.57 \qquad (J/m^2)$$

$$\lambda_{gb} = -0.000931T + 2.093 \qquad (J/m^2)$$

The minimum 90% confident prediction interval was 7.8%. The interfacial free energies of Ti-5Aℓ-2.5Sn were less than those determined in a previous study for pure Ti and Ti-6Aℓ-4V. These differences were explained thru equilibrium segregation of solutes to the interfaces. A relatively high grain boundary to surface free energy ratio for Ti-5Aℓ-2.5Sn, $\lambda_{gb}/\lambda_s = 0.46$, seemed to indicate a segregational preference for the surface.

Under the Nabarro-Herring mechanism of deformation enough information from the creep tests was available to determine self-diffusion coefficients for the alloy. The temperature dependence of the self-diffusion coefficient was fitted to the following Arrhenius expression in SI units:

$$D = 5.7(10^{-6}) \exp(-1.82(10^8)/RT) \qquad (m^2/s)$$

where: R = gas constant

Comparisons to previous self-diffusion studies show reasonable agreement.